University of Cincinnati

Date: 4/12/2018

I, Joshua N Bergbower, hereby submit this original work as part of the requirements for the degree of Master of Science in Geology.

It is entitled:

Trace and Rare Earth Element Chemistry of Fluorite from the Illinois-Kentucky Fluorspar District and its Implications for the Origins of Mineralizing Fluids

Student's name: **Joshua N Bergbower**

This work and its defense approved by:

Committee chair: Craig Dietsch, Ph.D.

Committee member: Andrew Czaja, Ph.D.

Committee member: Lewis Owen, Ph.D.

Committee member: John Rakovan, Ph.D.

Committee member: Jared Singer, Ph.D.

30430

Trace and Rare Earth Element Chemistry of Fluorite from the Illinois-Kentucky Fluorspar District and its Implications for the Origins of Mineralizing Fluids

A thesis submitted to the Graduate School of
The University of Cincinnati
In partial fulfilment of the requirements for the degree of

Master of Science

in the Department of Geology of the
McMicken College of Arts and Sciences
June 2018
by

Joshua N. Bergbower
B.S., Southern Illinois University Carbondale, 2015

Advisory Committee:
Craig Dietsch, Ph.D. – Committee Chair
Andy Czaja, Ph.D.
Lewis Owen, Ph.D.
John Rakovan, Ph.D.
Jared Singer, Ph.D.

Abstract

The Illinois-Kentucky Fluorspar District (IKFD) is a fluoritic sub-type of a Mississippi Valley Type (MVT) deposit characterized by the District's abundance of fluorite compared to minor Pb-Zn mineralization. Found along the axis of the District are a host of Permian ultramafic dikes, pipes, and diatremes, and Hicks Dome, a cryptoexplosive structure formed by the release of magmatic volatiles from a carbonatite complex intruded into Precambrian basement. Below the center of Hicks Dome is a large breccia deposit enriched in fluorite and REEs that are principally contained in secondary REE-bearing phosphate and fluorocarbonate minerals. Decreasing fluid inclusion temperatures and changes in fluorite chemistry from Hicks Dome to the fringes of the District indicate heating of the regional MVT system from magmatic activity at Hicks Dome. Previous studies support a model for magmatic gases lowering fluid pH, supplying fluorine, and brecciating country rocks. Fluid inclusion studies in fluorite show the presence of two distinct mineralizing fluids: a lower temperature-higher salinity fluid in paragenetically early fluorite, and a higher temperature-lower salinity fluid in later fluorite.

The REE and other selected trace element chemistry of over 530 fluorite samples from 32 locations across the District was analyzed in this study using LA-ICP-MS. Chondrite normalized REE patterns of early F1 fluorite are depleted in LREEs, have nearly flat to gently negative sloping HREEs, and can have a small positive Gd anomaly. REE patterns of late F2 fluorite are similarly depleted in LREEs, show small MREE enrichment, similar to more steeply negative HREEs, and a positive Eu anomaly. REE concentrations are similar between the two patterns, typically 10x chondrite or less. With a few exceptions there is an overall decrease in REE concentration with increasing distance from Hicks Dome. Neither early nor later fluorite has REE patterns similar to fluorite from a mineralized fracture within the ultramafic Sparks Hill diatreme, characterized by

LREE enrichment and a pattern sloping from La to Lu. This pattern is similar to whole rock REE patterns of the Sparks Hill diatreme and other intrusive rocks within the IKFD. Data obtained in this study suggest little REE input from magmatic fluids into the regional MVT system.

Acknowledgements

I would like to dedicate this work to my sisters, Breanna and Mallory, my parents, Gery and Charlene, and my grandparents, Lorene, Betty, and Cornelius for their constant support and encouragement throughout my pursuit of higher education.

I want to start by thanking my advisor Dr. Craig Dietsch. His knowledge, creativity, positivity, friendship, and guidance were instrumental to the success of this project and to my pursuit of advancing my knowledge of economic geology.

I would like to thank my committee members for their revisions and contributions to my thesis. A special thanks to F. Brett Denny and Joe Devera of the Illinois State Geological Survey for their expertise of the geology of Illinois, for supplying the extensive collection of fluorite samples that were analyzed in this study, and for laying the groundwork that this project was built on. Thanks to my friend Christopher Ely for his ability to navigate the woods of southern Illinois and whom with I spent many hours in the field collecting samples. Thanks to Warren Anderson of the Kentucky Geological Survey for his thorough knowledge of the geology of Kentucky and for supplying additional samples. Thanks to Dr. John Rakovan for his insights on the Illinois-Kentucky Fluorspar District and the chemistry of fluorite and the rare earth elements. And thanks to Dr. Jared Singer for his vast knowledge of analytical techniques, his dedication to understanding the intricacies of fluorite ablation, and to the many hours spent in the lab preparing, testing, and analyzing samples.

Thanks to the Department of Geology at the University of Cincinnati, where my many friends and colleagues provided me with the support and resources needed to succeed. Lastly, thanks to Sigma Xi, the Geological Society of America, and the Society of Economic Geologists for their financial support, without which this project could not have been completed.

Table of Contents

List of Tables

List of Figures

Chapter 1: Introduction

The Illinois-Kentucky Fluorspar District (IKFD) has been historically, the most prolific producer of fluorite within the United States. Production occurred for over 175 years from over 200 mines until the last mine closed in 1995 (Goldstein, 1997). In recent years, however, the District has been looked at as a potential source of rare earth elements (REEs). With the emergence of both civilian and military electronic devices and electric vehicles whose components rely on the use of REEs, REEs have become societally significant. In 2014, China was the world's largest producer and exporter of REEs accounting for over 84% of global production (U.S. Geological Survey, 2014). Uncertainty in political and economic relations with China gives REEs from within the United States economic and strategic importance.

The IKFD has been classified as a Mississippi Valley Type (MVT) deposit based on its mineralogy, mineralization style, and fluid inclusion temperatures and salinities (Heyl et al., 1974), but the IKFD has some significant differences compared to a typical MVT deposit. MVT deposits are found throughout the world, but the largest deposits occur in North America (Leach et al., 2010). Leach et al. (2005) (cited in Leach et al., 2010) summarize an MVT deposit as follows:

> *(1) they are epigenetic; (2) they are not associated with igneous activity; (3) they are hosted mainly by dolostone and limestone, rarely in sandstone; (4) the dominant minerals are sphalerite, galena, pyrite, marcasite, dolomite, and calcite, whereas barite is typically minor to absent and fluorite is rare; (5) they occur in platform carbonate sequences commonly along the flanks of basins or foreland thrust belts; (6) they are commonly stratabound but may be locally stratiform; (7) they typically occur in large districts; (8) the ore fluids were basinal brines with ~10 to 30 wt. percent salts; (9) they have crustal sources for metals and sulfur; (10) temperatures of ore deposition are typically 75°C to*

about 200°C; (11) the most important ore controls are faults and fractures, dissolution collapse breccias, and lithological transitions; (12) sulfides are coarsely crystalline to fine grained, massive to disseminated; (13) sulfides occur mainly as replacement of carbonate rocks and to a lesser extent, open-space fill; and (14) alteration consists mainly of dolomitization, host-rock dissolution, and brecciation.

The IKFD differs markedly in that the District contains intrusive igneous rocks, fluorite mineralization predominates, sulfide mineralization is only minor, and a large number of vein deposits occur throughout the District. The IKFD appears to be a hybrid deposit, best classified as a fluoritic sub-type of a MVT deposit (Rakovan, 2006). Similar deposits are found in Central Tennessee and the English Pennines. Although the IKFD has been studied for decades, there are still several questions remaining about the formation of fluorite and rare earth element mineralization in the District.

Numerous studies indicate that IKFD mineralizing fluids originated as connate basinal brines driven northward from deep Paleozoic aquifers within the Reelfoot Rift (e.g., Hall and Friedman, 1963; Heyl et al., 1974; Cunningham and Heyl, 1980; Richardson and Pinckney, 1984; Leach et al., 1997; Rowan and de Marsily, 2001; Kendrick et al., 2002a; Pelch et al., 2015). Fluid inclusions in IKFD fluorite are of similar temperature and salinity to fluids responsible for the formation of other MVT deposits (Leach et al., 2010). However, work done by several authors indicate that mantle-derived intrusive igneous activity beneath Hicks Dome supplied heat (Taylor et al., 1992), fluorine (Plumlee et al., 1995), trace elements (Hall and Heyl, 1968; Heyl et al., 1974), and REEs (Burruss et al., 1992) to the regional MVT fluids before they reached sites of ore deposition. Plumlee et al. (1995), using fluid inclusion and trace element data obtained from several studies, developed a model in which the basinal brines were drawn into a thermal convective system underlying Hicks Dome to explain IKFD mineralization. Here, HF-rich magmatic gases mixed with the regional basinal brines, producing fluids with dissolved F, before these modified fluids rose along major faults where cooling, fluid mixing, and reactions with carbonate rocks drove fluorite mineralization.

The purpose of this study is to analyze the rare earth element and trace element chemistry of fluorite sampled from across the IKFD and use these data to test whether fluorine, REEs, and increased heat were sourced from the injection of magmatic fluids into the regional MVT system at Hicks Dome (e.g., Heyl et al., 1974; Cunningham and Heyl, 1980; Burruss et al., 1992) or whether fluorine was mobilized through the dissolution of F-rich igneous gases into regional MVT fluids (Plumlee et al., 1995). In this case, the REEs in fluorite were sourced from sedimentary rocks with the addition of remobilized REEs from the intrusive igneous rocks in the District. In addition, this study aims to determine whether REE-bearing mineralization associated with fluorite is restricted in occurrence to the Hicks Dome breccia.

The REE and selected trace element chemistry of over five hundred and thirty individual fluorite grains from thirty-two mine and prospect pit locations across the District were measured. Results show that overall REE abundances are low, with Y being the only REE to generally exceed concentrations of 10 ppm. The data show the presence of two distinct REE patterns: one pattern is found in paragenetically early fluorite while the other pattern is found in paragenetically later fluorite. Chondrite normalized REE patterns show light REE depletion, medium REE enrichment, and varying degrees of heavy REE depletion with all samples having a distinct positive Y anomaly.

Chapter 2: Geologic Setting of the IKFD

The IKFD lies at the southern end of the Illinois Basin near the Basin's depocenter. The southern end of the Basin was open to sedimentation until its closure in the late Paleozoic due to uplift of the Pascola Arch (Bethke, 1986; Kolata and Nelson, 1991). Sedimentation in the Illinois Basin began in the Late Cambrian and continued intermittently into the Permian, accumulating more than 4,000 m of sedimentary rocks in the basin depocenter (Bethke, 1986; Kolata and Nelson, 1991). Exposed at the surface are relatively flat lying Lower Pennsylvanian sandstones and shales unconformably overlying Mississippian sediments. The Upper Mississippian is composed of limestone, sandstone, and shale, the Lower Mississippian of limestone and dolostone, and the oldest Mississippian units are made up of dark, organic-rich shale of the New Albany group that extends down into the Upper Devonian. Below the New Albany, but not exposed in the District, are older Devonian, Ordovician, and Cambrian sedimentary strata. The Paleozoic units lie unconformably on Precambrian basement of the 1.4–1.5 Ga Eastern Granite-Rhyolite province (Van Schmus et al., 1996).

2.1 Tectonics

Some of the structural features of major importance in the IKFD include the Reelfoot Rift/Rough Creek Graben, the Fluorspar Area Fault Complex, the Tolu Arch, and Hicks Dome (Figs. 1, 2, and 3).

Structurally, the IKFD is located in the northwestern corner of the Reelfoot Rift/Rough Creek Graben. The Reelfoot Rift is an aulocogen (a failed rift) that resulted from the breakup of the supercontinent Rodina in the late Precambrian (Nelson, 1995). The Reelfoot Rift extends from the Ouachita fold belt in Arkansas northeastwards into western Kentucky, where it turns abruptly eastward to form the Rough Creek Graben, and continues directly east further into Kentucky (Nelson, 1991) (Fig. 1). The Reelfoot Rift and Rough Creek Graben are bounded on both sides by large listric normal faults that cut into the Precambrian basement (Nelson, 1995; Potter et al., 1995). These normal faults were periodically reactivated throughout the Paleozoic. By the end of the Paleozoic, subsidence within the rift is estimated to have allowed upwards of 7,000 m of sediments to be deposited (Leach et al., 1997). Due to late Paleozoic uplift and erosion, and subsequent renewed sedimentation, the youngest rocks exposed in the rift are Cretaceous-Tertiary rocks unconformably overlying Paleozoic rocks (Leach et al., 1997; Rowan and de Marsily, 2001).

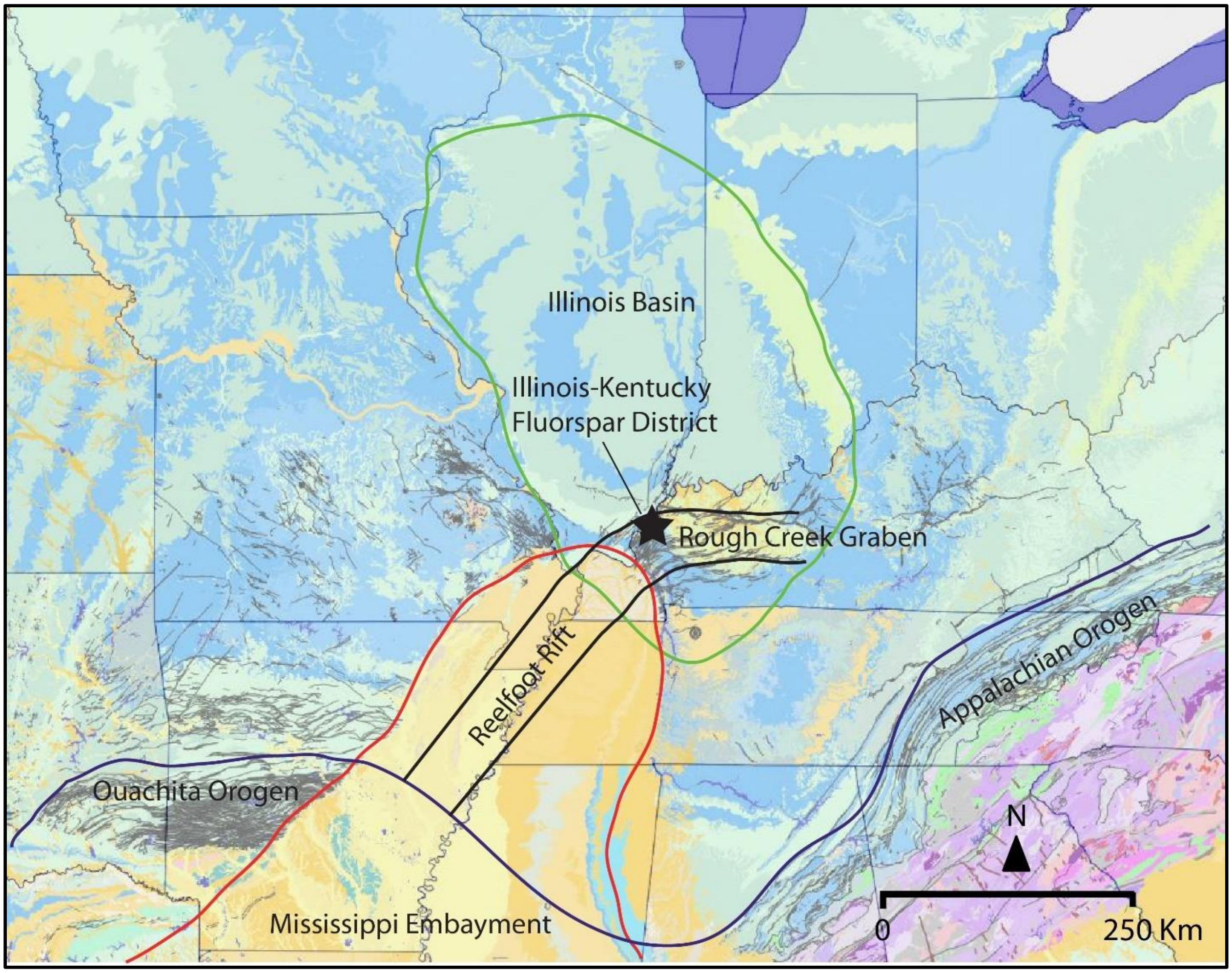

Figure 1. Map showing the location of the Illinois-Kentucky Fluorspar District. The Illinois Basin is outlined in green, the Reelfoot Rift and Rough Creek Graben in black, the Mississippi Embayment in red, and the Appalachian-Ouachita Orogen in purple. Data acquired from the USGS Mineral Resources Online Spatial Data. (Subsequent figures of the IKFD are centered on the star.)

The IKFD is located amid the Fluorspar Area Fault Complex (FAFC), considered to be the most complexly faulted area in the North American midcontinent (Nelson, 1995) (Fig. 2). The FAFC is located within the bend of the Reelfoot Rift/Rough Creek Graben and is bounded to the north by the Rough Creek-Shawneetown Fault System (Nelson, 1991) and to the south by the Pennyrile Fault System (Potter et al., 1995) (Fig. 1). In between these two bounding faults, the

FAFC is made up of dozens of northeast-trending faults, many of which host the District's fluorite mineralization. These faults are primarily high-angle normal, with some known reverse faults, and even indications of strike-slip movement occur on some of them (Nelson, 1995). The complex faulting of the area produced many horsts and grabens, of which the grabens appear to have acted as controls on mineralization. Some deposits show evidence that fault movement occurred after fluorite mineralization (Bastin, 1931; Currier and Wagner, 1944).

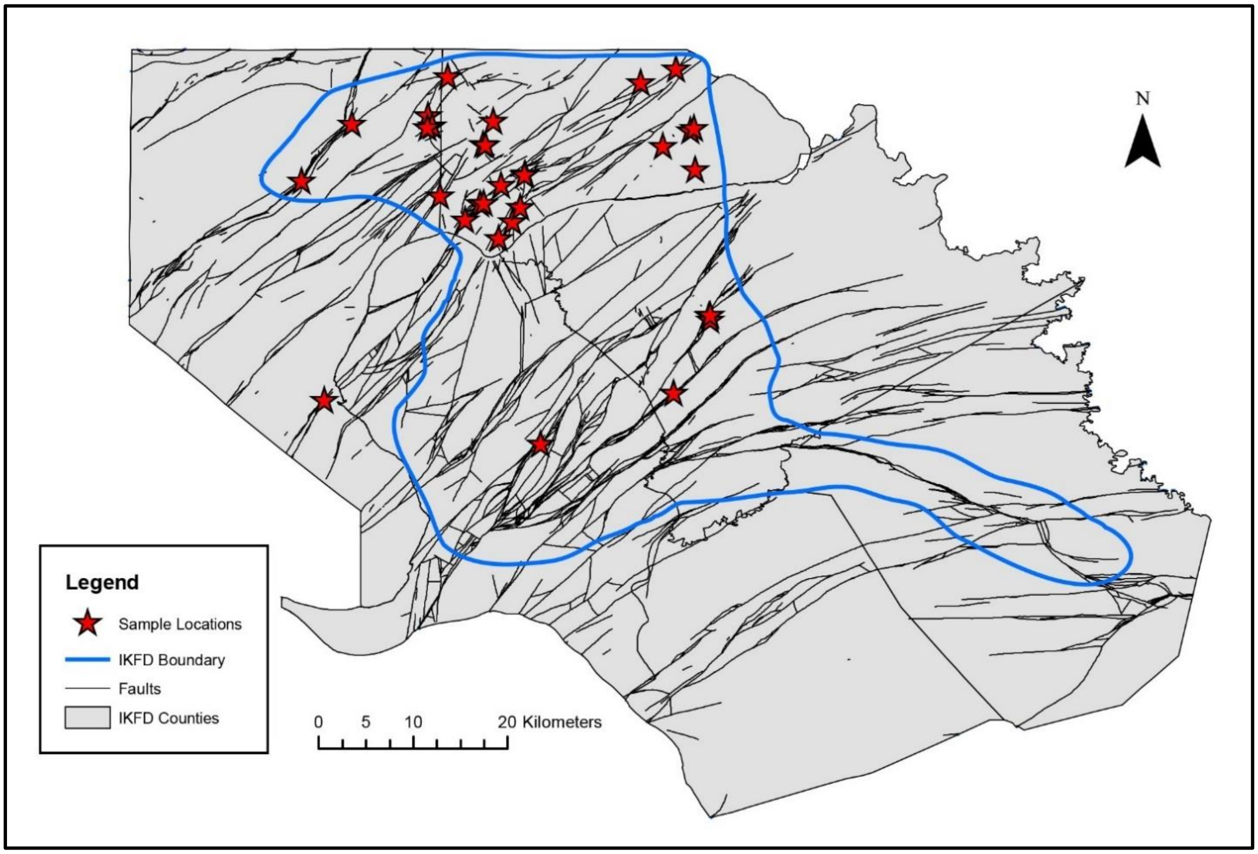

Figure 2. Map showing the Illinois-Kentucky Fluorspar District, locations of samples analyzed in this study, and major structural features of the region.

2.2 Intrusive Rocks and Hicks Dome

The Tolu Arch, thought to be a partially collapsed magmatic or explosive volcanic uplift, extends from Kentucky into Hardin County, Illinois, and is broken up into many blocks by the faults of the FAFC (Nelson, 1995) (Figs. 2 and 3). Aligned along the crest of the Tolu Arch are many northwest-trending mantle-derived igneous dikes, pipes, and diatremes (Bradbury and Baxter, 1992) (Fig. 3). Based on ^{40}Ar/^{39}Ar ages of phlogopite and hornblende found in intrusive breccias, the intrusive rocks crystallized at approximately 270 Ma (Snee and Hayes, 1992; Reynolds et al., 1997; Fifarek et al., 2001; Denny, 2005).

At the northern end of the district in Illinois and along the apex of the Tolu Arch, lies Hicks Dome (Fig. 3). Hicks Dome, defined by an oval shaped outcrop pattern of the New Albany shale, elongated northwest-southeast, is approximately 16 km in diameter, and has an estimated 1,200 m of vertical uplift (Nelson, 1991). Hicks Dome was initially believed to be a cryptovolcanic structure, due to the numerous dikes, pipes, and breccias that radiate from the dome, but due to the lack of extrusive igneous rocks at the surface it is now thought to be more accurately termed a cryptoexplosive structure (Bradbury and Baxter, 1992; Nelson 1995; Denny et al., 2015), formed by the explosive release of igneous volatiles from an intrusion at depth (Bradbury and Baxter, 1992; Potter et al., 1995). Seismic data from across the dome indicate that not only is a 6.1 km thick sequence of sedimentary beds uplifted, but the top of the Precambrian basement is also domed (Potter et al., 1995). Seismic reflections in the basement up through the Cambrian-Ordovician section are extremely disrupted and have been interpreted to mean the intrusive body responsible for uplift of the dome lies lower in the Precambrian basement and not in the sedimentary section (Potter et al., 1995). Another line of evidence supporting an explosive release of igneous volatiles at Hicks Dome is the occurrence of pelletal lapilli in some of the intrusive rocks (Denny, 2005). These lapilli, restricted in occurrence to ultramafic pipes, are made up of clasts surrounded by a rim of rapidly cooled juvenile melt, possibly the result of fluidized spray granulation (Gernon et al., 2012).

The intrusive rocks at Hicks Dome have mineralogical and isotopic signatures distinct from other intrusive rocks throughout the IKFD. The intrusive rocks at Hicks Dome, although extensively altered by hydrothermal fluids, fit closely with the classification of calc-alkaline lamprophyre and are defined precisely as minette, while other intrusive rocks in the District are classified as ultramafic lamprophyres (Moorehead, 2013). Hicks Dome intrusive rocks have higher carbonate contents (13–21 weight % CO_2) and lower silica contents (23–25 weight % SiO_2) compared to other igneous samples across the region (1–2 weight % CO_2 and 33–36 weight % SiO_2; Moorehead, 2013). Whole rock REE patterns of intrusive rocks throughout the District show that the rocks at Hicks Dome have steeper and more elevated concentrations of REEs, 473.0 ppm La and 0.8 ppm Lu on average, similar to those of carbonatites, compared to average values of 91.8 ppm La and 0.2 ppm Lu for other samples (Moorehead, 2013).

The Henry Hamp, Jr. No. 1 exploration well, drilled at the top of Hicks Dome, encountered the expected sequence of Paleozoic formations to 1,600 ft where the drill intersected a heavily brecciated zone that continued to the bottom of the hole at 2,944 ft (Brown et al., 1954). This breccia (designated the Hicks Dome breccia in this study) is cemented with fluorite, barite, calcite, quartz, pyrite, sphalerite, and galena, and contains abundant REE and Th-bearing minerals, including monazite, xenotime, fluorencite, and yttroparisite (Brown et al., 1954; Trace, 1960; Hall and Heyl, 1968). The fact that intrusive breccias closely associated with Hicks Dome contain either a carbonatite suite of elements (e.g., REE, Th, Nb, and Be) (Trace, 1960; Hall and Heyl, 1968; Baxter and Bradbury, 1980) or igneous rock and mineral fragments in a carbonate matrix, led Bradbury and Baxter (1992) to conclude that Hicks Dome is a carbonatite complex.

Carbonatites contain the highest concentrations of REEs of all rock types (Cullers and Graf, 1984), and can contain volatiles that include CO_2, H_2O, Cl, F, and S (Verplanck et al., 2016).

According to Verplanck et al. (2014), carbonatites are typically part of larger magmatic complexes, and the concentration of REEs is believed to be linked to alkaline magmas that undergo extreme fractional crystallization as they ascend through the crust. Fractional crystallization concentrates volatiles and incompatible elements in the residual magma, and they can exsolve as a separate fluid phase (Verplanck et al., 2016).

Although intrusive activity occurs all along the axis of the District, likely resulting from late Paleozoic regional extension and subsequent partial melting of the underlying mantle (Fifarek et al., 2001), the evidence indicates that the intrusive rocks at Hicks Dome formed from a magma that was enriched in trace elements, REEs, and volatiles relative to igneous rocks elsewhere in the District. Hicks Dome is an unusual area in the IKFD in that there is explosive uplift and unique mineralization.

Chapter 3: Fluorite Mineralization

3.1 Types of Fluorite Deposits in the IKFD

The IKFD is known for its extensive fluorite mineralization. Other minerals commonly found in the District include calcite, barite, quartz, galena, and sphalerite. There are 4 types of fluorite deposits found throughout the District: vein, bedding replacement, solution-slump breccias, and fluorite-cemented explosion breccias. Examples of the first three types of fluorite deposits have been described by many authors (e.g., Bain, 1905; Bastin, 1932; Currier and Wagner, 1944; Grogan, 1949; Brecke, 1962; Goldstein 1997). The most common are vein deposits, where fluorite crystalizes from the movement of mineralizing fluids up faults and fractures, cooling and reacting with wall rocks. Bedding replacement deposits form from the lateral migration of mineralizing fluids through porous Mississippian carbonates where fluids dissolved the purer limestone beds and fluorite mineralization replaced them. Bedding replacement deposits are most commonly found in horsts on either side of the Rock Creek Graben, east of Hicks Dome. These are known as the Cave-in-Rock and Harris Creek subdistricts (Fig. 3); fluorite subdistricts are clusters of mines, typically along the same fault system. The Mississippian formations that host the bedded deposits are almost always overlain by a formation with an impermeable basal shale (Goldstein, 1997). Overlying shale is important in sealing off fissures which forces fluids to migrate laterally through more permeable beds.

Solution slump breccias formed through the ascent of large volumes of fluids along fissures and fractures into what become ore zones where large amounts of carbonate dissolve, resulting in the overlying beds falling down or “slumping” into the cavity below. The overlying beds become fragmented and broken up as they slumped. Later, as more mineralizing fluids pass through, the remaining open spaces in these slump breccias are cemented with fluorite.

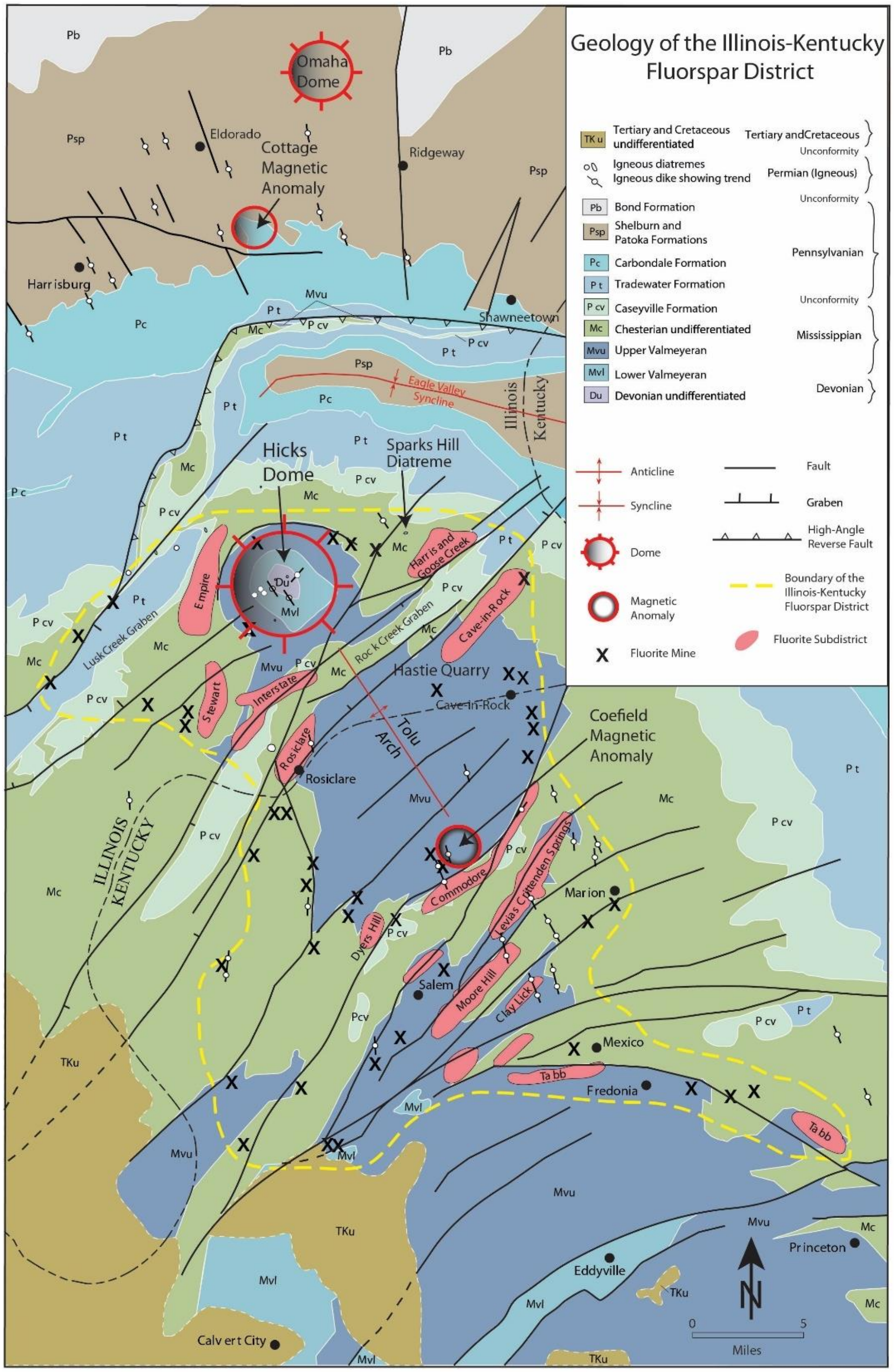

Figure 3. Map outlining the Illinois-Kentucky Fluorspar District. Major features include: fluorite subdistricts, Hicks Dome, the Tolu Arch, and igneous intrusions. Notice the fault-controlled nature of fluorite subdistricts (modified from Denny et al., 2008).

3.1.1 Fluorite Cemented Explosion Breccias

The fourth style of mineralization is restricted to rocks near and beneath Hicks Dome (Bradbury and Baxter, 1992). During the formation of Hicks Dome, distinct zones and pipes of brecciation and diatremes were formed. Breccias contain both host rock clasts and igneous xenocrysts and xenoliths (Bradbury and Baxter, 1992). Over 40 breccia pipes are known to occur in the Hicks Dome area, but only 7 are known to contain fluorite mineralization (Bradbury and Baxter, 1992). The Henry Hamp, Jr. No. 1 well, as mentioned above, intersected a large breccia body directly underneath Hicks Dome, that was found to be cemented with abundant low-grade fluorite and REE-bearing phosphate (e.g., florencite and xenotime) and fluorocarbonate (e.g., synchysite and parasite) minerals (Brown et al., 1954; Trace, 1960; Hall and Heyl, 1968).

Office of Minerals Explorations (OME) project 6873, operated by the Department of Interior in collaboration with the U.S. Geological Survey in the 1970s, found that the Hicks Dome breccia contained an estimated 10 to 20 million tons of rock containing 8 to 22% fluorite (U.S. Geological Survey, 1978). The highest-grade mineralization was found to occur at a depth of 1800 to 2200 ft in a 180 to 200 ft thick zone of purple replacement fluorite and cement within breccia fragments of the Ordovician Plattin limestone (U.S. Geological Survey, 1978). Breccia fragments are very fine grained, described as rock flour, down to the base of the Plattin limestone where there is a sharp contact. Below this contact, the breccia body is predominantly made up of large fragments. By drilling several more holes at the top of Hicks Dome, the project geologist was able to determine that the Hicks Dome breccia extended over 1200 ft laterally east to west, and over 2000 ft vertically, resembling the shape of an inverted funnel. The central core of the breccia was found to be sparsely mineralized by angular fragments of dark purple fluorite that appear to record a second, post-mineralization brecciation that disrupted the central zone of the breccia body (U.S. Geological Survey, 1978).

3.2 Paragenetic Sequences and the Age of Fluorite Mineralization

The bedding replacement ores of the Cave-in-Rock and Harris Creek subdistricts on either side of the Rock Creek Graben are the most thoroughly studied. A generalized paragenetic sequence for the Cave-in-Rock subdistrict was established by Richardson and Pinkney (1984) and later updated by Spry and Fuhrmann (1994) to cover all bedding replacement deposits in the IKFD (Fig. 4). The early paragenesis is made up of an alternating sequence of yellow and purple fluorite. Mineralization thereafter was predominantly bands of purple, blue, and clear fluorite, which was followed by calcite, barite, and witherite mineralization. Sulfide mineralization, although not found in all mines, is restricted to the middle stages of the paragenesis (Fig. 4) during which time chalcopyrite inclusions commonly formed within fluorite crystals. Portions of this complete paragenetic sequence were correlated to vein deposits in Kentucky, indicating regionwide interconnected fluid flow (Hayes and Anderson, 1992).

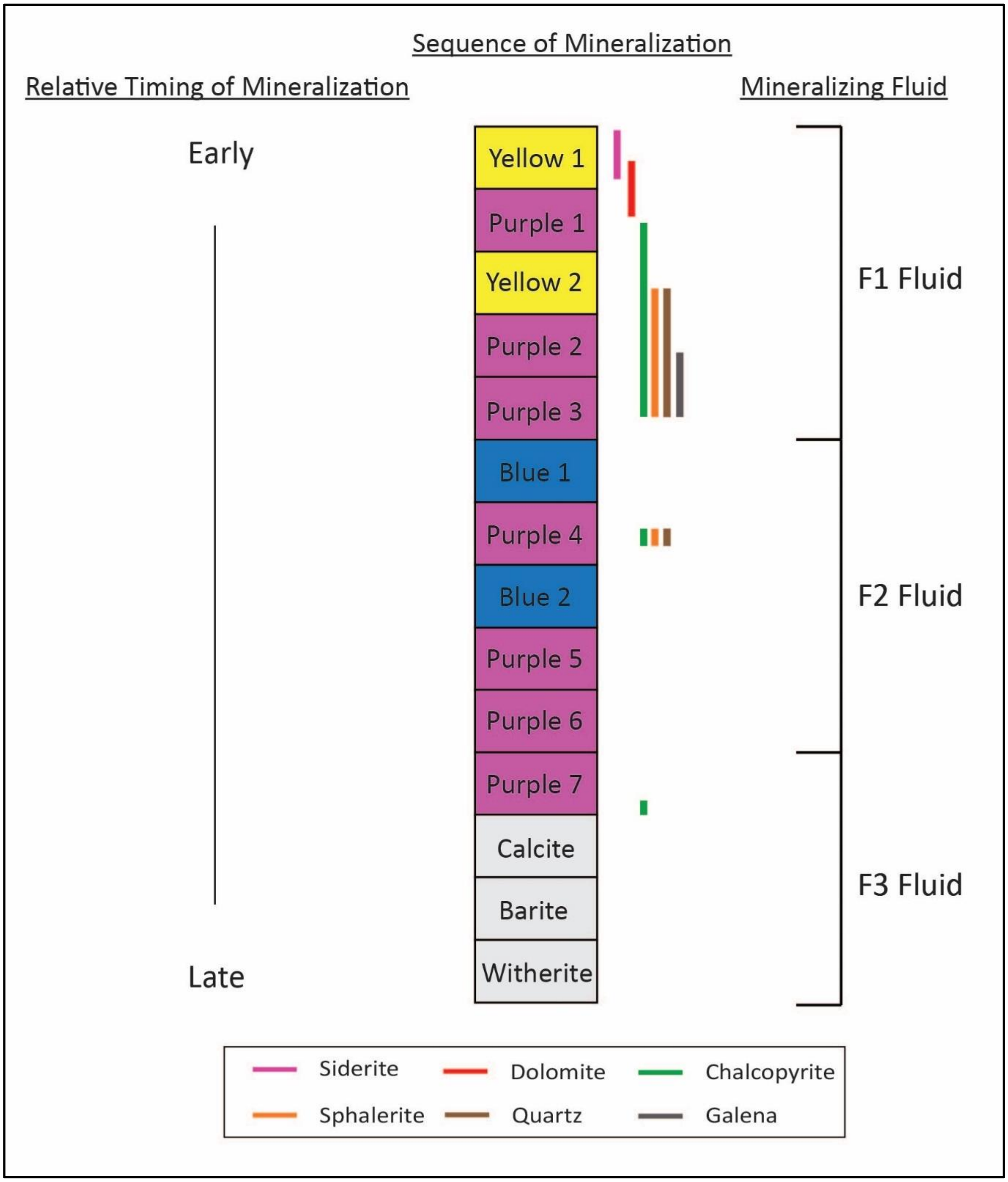

Figure 4. Generalized paragenetic sequence of fluorite and associated minerals within the bedding replacement deposits of the Harris Creek and Cave-in-Rock subdistricts (modified from Spry and Fuhrmann, 1994).

Several attempts have been made to date fluorite mineralization in the IKFD. Ruiz et al. (1988) determined an Early Jurassic age using $^{87}Sr/^{86}Sr$ ratios of fluorite from the Cave-in-Rock subdistrict. Symons (1994) used paleomagnetic analysis on both ore and host rock to determine a Late Jurassic age. Brannon et al. (1996) measured $^{232}Th/^{208}Pb$ and $^{238}U/^{206}Pb$ ratios in ore stage calcite and reported ages of 194 ± 13 Ma and 195 ± 23 Ma, respectively. Harder (1987) (cited in Symons, 1994) used fission track dating on fluorite to determine ages of 135.7 ± 4.5 Ma and 140.6 ± 4.7 Ma. Chesley et al. (1994) used $^{147}Sm/^{144}Nd$ ratios of fluorite samples from 3 mines in the Cave-in-Rock subdistrict to determine a Permian age of 272 ± 17 Ma, in agreement with $^{40}Ar/^{39}Ar$ age data of hornblende and biotite from the Grants Intrusive breccia at Hicks Dome (Snee and Hayes 1992). Although there are substantial differences among these age data, several lines of evidence indicate that the timing of fluorite mineralization likely occurred in the Permian.

A Permian age of fluorite mineralization in the IKFD is supported by Permian ages of sphalerite mineralization in the Upper Mississippi Valley (UMV) District located at the northern end of the Illinois Basin. The UMV District is more typical of a MVT deposit in that it contains economic Pb and Zn mineralization and is not overprinted by magmatic activity. Rb-Sr dating of sphalerite gave an age of 270 ± 4 Ma (Brannon et al., 1992). Like the IKFD, mineralizing fluids of the UMV are believed to have been sourced from the Reelfoot Rift (Rowan and Goldhaber, 1996; Rowan and de Marsily, 2001). Uplift of the Ouachita fold belt at the southern end of the Reelfoot Rift is known to have begun during Late Pennsylvanian/Early Permian time, producing the topographic relief needed to drive fluids out of the Reelfoot Rift northward through the Illinois Basin (Rowan and Goldhaber, 1996) (Fig. 5). If a Permian age of mineralization is correct, then mineralization in the IKFD and the UMV appears to have occurred contemporaneously. Another line of evidence for Permian mineralization is that fluorite from across the IKFD contains numerous oil-bearing inclusions (e.g., Richardson and Pinckney, 1984; Spry and Fuhrmann, 1994). Cluff and Byrnes (1990) used current maturation and vitrinite reflectance data in conjunction with a Lopatin model to predict oil and gas maturation windows for the New Albany shale. They determined that maturation and northward migration of petroleum from the New Albany shale in the southern end of the basin likely occurred in the Late Paleozoic. In addition, the carbonatite and lamprophyre intrusions, with ages of 270 Ma, have been linked to fluorite mineralization by supplying fluorine, fluid pH, and heat (e.g., Plumlee et al., 1995).

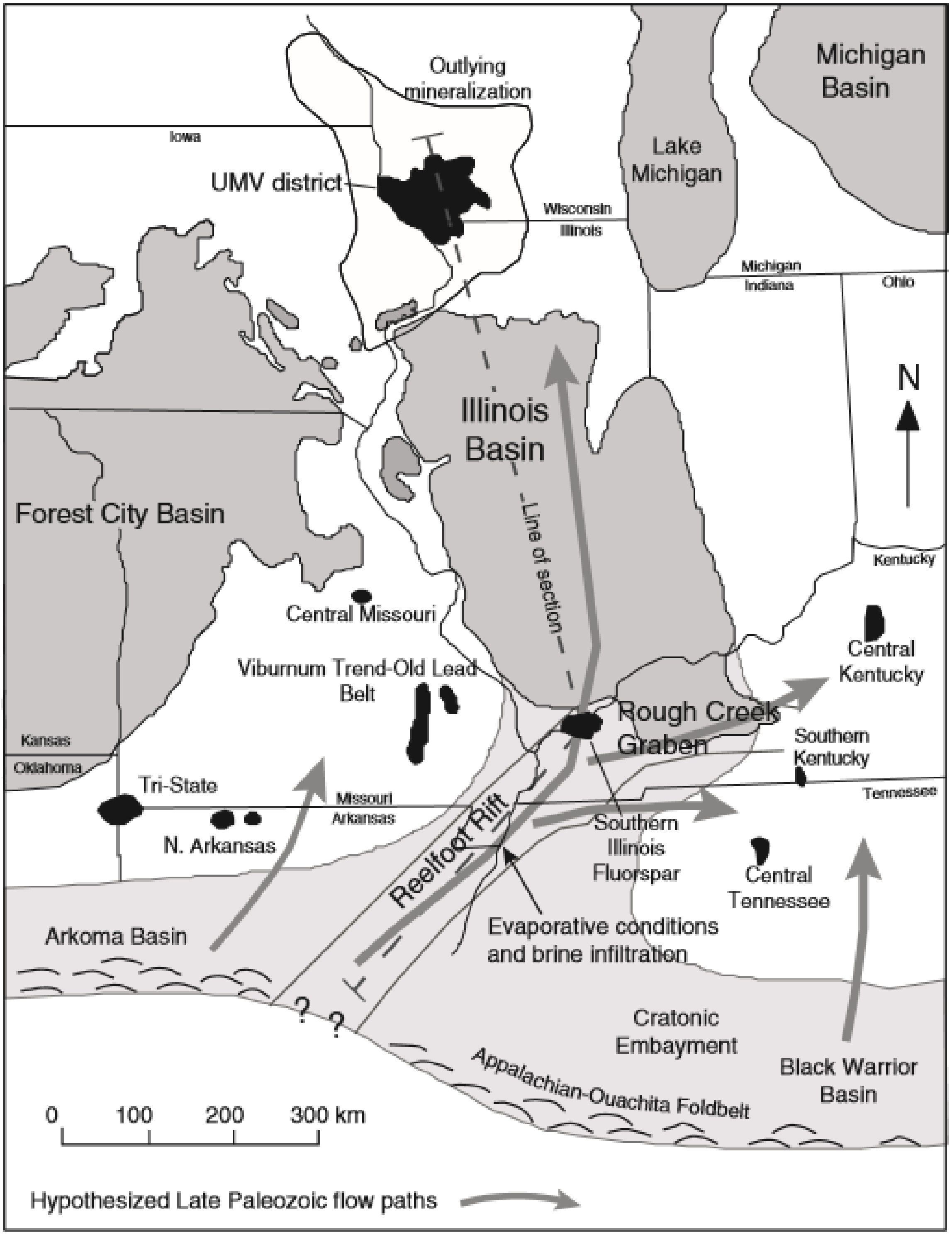

Figure 5. Map showing hypothesized fluid flow direction northward out of the Reelfoot Rift and across the Illinois basin (unmodified from Rowan and de Marsily, 2001).

3.3 Mineralizing Fluid Characteristics

Fluorite fluid inclusion compositions have been thoroughly studied (e.g., Hall and Friedman, 1963; Richardson and Pinckney, 1984, Richardson et al., 1988; Spry et al., 1990; Taylor et al., 1992; Spry and Fuhrmann, 1994; Kendrick et al., 2002a; Pelch et al., 2015). Two primary mineralizing fluids of similar composition and a distinctive late-stage meteoric fluid have been identified. Spry and Fuhrmann (1994) found fluid inclusion data from several bedding replacement deposits to indicate the presence of two mineralizing fluids for the formation of fluorite. Their fluid 1 (F1) is a lower temperature-higher salinity mineralizing fluid – estimated to have been at conditions of <125°C and 23 weight % NaCl equivalent – that is present in paragenetically early fluorite (yellow 1 through purple 3, Fig. 4) fluid inclusions. Fluid 2 (F2) is a higher temperature-lower salinity mineralizing fluid – at conditions of 150°C and 19 weight % NaCl equivalent – in paragenetically late fluorite (blue 1 through pre-purple 7, Fig. 4). The authors found evidence that these fluids may have mixed to varying degrees at the site of ore deposition. Cunningham and Heyl (1980) found fluid inclusions within post-fluorite mineralization quartz, barite, and witherite to be significantly more dilute, with smaller deuterium-hydrogen ratios, and increased sulfate content compared to fluorite, indicating late-stage input of a lower temperature, lower salinity meteoric water at the end of fluorite mineralization (Hall and Friedman, 1963; Richardson and Pinckney, 1984; Richardson et al., 1988).

3.3.1 Sources of Mineralizing Fluids

Pelch et al. (2015) determined that fluid inclusions in the IKFD contain higher atomic ratios of Ba/Na, Ca/Mg, K/Na, and Sr/Na, and lower atomic ratios of Mg/Na compared to inclusions within neighboring Ozark MVT Districts. They concluded that the ore fluids were compositionally distinct and therefore originated from different source basins. Pb isotopes in galena from the Illinois Basin were also found to have vastly different ratios than those of the Ozark MVT Districts (Goldhaber et al., 1994), further supporting the model that mineralizing fluids were sourced from different basins.

It is generally agreed upon that the source of most basinal brines is sedimentary formation water, and their high salinities are acquired primarily through subaerial seawater evaporation and the subsequent concentration of dissolved ions; while dissolution of evaporites appears to have played a minor role in concentrating salinities in many districts (Rowan and de Marsily, 2001). Kendrick et al. (2002a) found evaporation of seawater beyond the point of halite saturation, subsequently diluted to varying degrees by meteoric water, to be the most likely source of MVT ore fluids. During sedimentation of the Reelfoot Rift, the conditions were likely adequate for formation of a well saturated brine, driven by evaporation, that could then percolate down and mix with the fluids in the underlying sandstone aquifers in areas of adequate permeability (Rowan and de Marsily, 2001).

The Illinois Basin contains two sandstone formations, the Mt. Simon and St. Peter, whose exceptionally high porosities and permeabilities could accommodate large volumes of lateral fluid flow (Bethke et al., 1991); both formations are continuous across the Basin. The Cambrian Mt. Simon Sandstone is a basal sandstone lying unconformably on Precambrian basement and is stratigraphically continuous across the Illinois Basin into the Reelfoot Rift (Rowan and de Marsily, 2001). The Ordovician St. Peter Sandstone could also have acted as a major aquifer for fluid flow across the Illinois Basin (Pitman et al., 1997). Fluid inclusion homogenization temperatures within dolomite cement less than 150 m above the Mt. Simon Sandstone have been found to range from 150–280°C and to have salinities consistent with those found within fluorite inclusions, 18–23 weight % NaCl equivalent (Leach et al., 1997). The dolomite cements are believed to have mineralized from basinal brines flowing through the Reelfoot Rift (Leach et al., 1997).

Goldhaber et al., (1994) used fluorine concentrations from Ordovician carbonates, stratigraphically above and below the St. Peter Sandstone aquifer, as a tracer for brine migrations within the Illinois Basin. Concentrations of fluorine in individual wells increased with proximity to the St. Peter Sandstone, indicating that it could have been a major migration pathway for fluids across the basin. Pb isotopes from the UMV, the IKFD, epigenetic pyrite in wells between the two districts, Cambro-Ordovician carbonates of the southern part of the basin, and from epigenetic sulfides in the Reelfoot Rift all fall along the same isotopic trend, thus indicating large-scale regional fluid flow (Goldhaber et al., 1994). Gravity driven migration of basinal brines is quite possible within Illinois Basin aquifers and has been proposed as the transport mechanisms for fluids through, or out of, other basins within the North American midcontinent (Garven et al., 1993).

The fluids responsible for fluorite mineralization within the IKFD are of similar temperatures and salinities to basinal brines responsible for forming other MVT deposits (Leach et al., 2010); the most striking difference, however, is the large concentrations of fluorine within IKFD fluids. Plumlee et al. (1995) gathered data on fluorite fluid inclusion composition in order to model the role of magmatic volatiles on fluorite mineralization. They believed CO_2- and HF-rich gases exsolving from the carbonatite magma likely mixed with regional basinal brines at depth. The modified basinal brines would become highly acidic, with an estimated pH of <3, where fluorine solubility is highest (Richardson and Holland, 1979). As the modified brines moved up along faults, boiling may have occurred due to decreasing pressure, but according to modeling by

Plumlee et al. (1995), the most likely drivers of fluorite mineralization would be reactions with calcium-rich carbonate host rocks and cooling of mineralizing fluids.

Kendrick et al. (2002a) determined the presence of 5–6% mantle-sourced helium within fluid inclusions from the IKFD, indicating a contribution of mantle volatiles to the system. Geochemical analysis on brines from over 100 wells in the southernmost part of the Illinois basin and 14 other wells dispersed across the basin indicated there is a fluorine-enriched region to the south of the Iowa-Missouri border and decreasing fluorine content away from Hicks Dome (Goldhaber et al., 1994).

3.3.2 The Hicks Dome Thermal High

Cunningham and Heyl (1980) measured homogenization temperatures of 175°C from fluorite and barite at the top of the Hicks Dome breccia, and 220 to 270°C in barite at 713 meters depth in the breccia, while Taylor et al. (1992) measured homogenization temperatures in fluid inclusions from 17 mines spanning the limits of the IKFD (Fig. 6). They determined high salinities in samples across the District and throughout the fluorite paragenesis, in addition to a distinct decrease in average temperature away from the center of Hicks dome (175°C) to the flanks of the dome (150°C) to the Cave-in-Rock subdistrict (132–150°C) to the southern fringes of the District (35–119°C) (Taylor et al., 1992). The combination of analytical error and the large range of fluid inclusion homogenization temperatures within samples from the same location are unlikely to support distinct isotherms radiating outwards from Hicks Dome, however, evidence from these studies undoubtedly suggests a thermal high around Hicks Dome and an overall decrease in fluid temperatures to the fringes of the district.

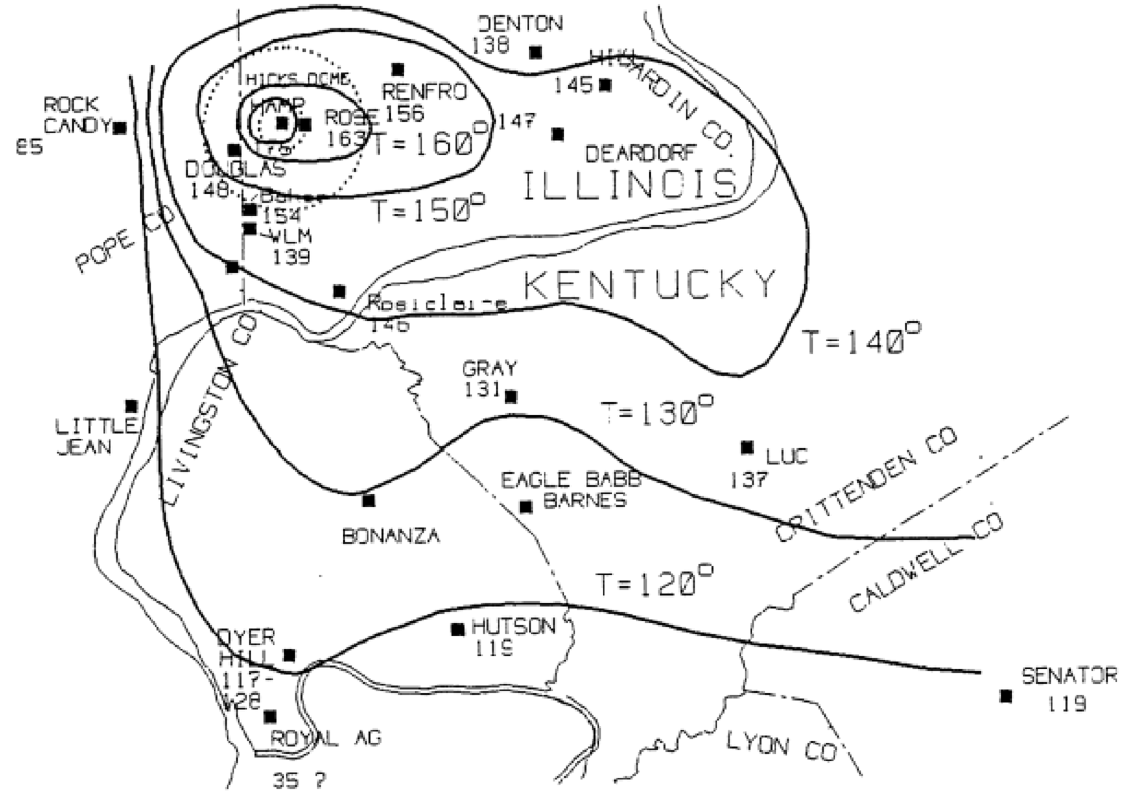

Figure 6. Map of fluid inclusion temperatures showing a thermal zonation around Hicks Dome (unmodified from Taylor et al., 1992).

Chapter 4: Methods

4.1 Sampling Strategy

The vast majority of samples analyzed in this project are on loan from the Illinois State Geological Survey (ISGS), of which I helped to collect half during the summer of 2014 while working for the ISGS. Samples were gathered from known abandoned mine or prospect pit locations primarily on the Illinois side of the District. Samples were gathered from tailings piles in direct physical association with an abandoned mine shaft or pit, with care taken not to collect fluorite in crushed gravel that could have been used in building of mine roads. One sample from the Sparks Hill diatreme was also analyzed; this sample was obtained through F. Brett Denny of the ISGS. In addition, calcite from several locations was also analyzed; calcite was collected in concert with collecting fluorite.

Sample locations and their fluorites were chosen for analysis for three primary reasons: (1) to give the best geographic distribution of fluorite REE and trace element compositions across the IKFD, (2) to sample fluorite from deposits located along major faults, away from major faults, and from both vein and bedding replacement deposits, and (3) to show grain-to-grain variability from a single locality.

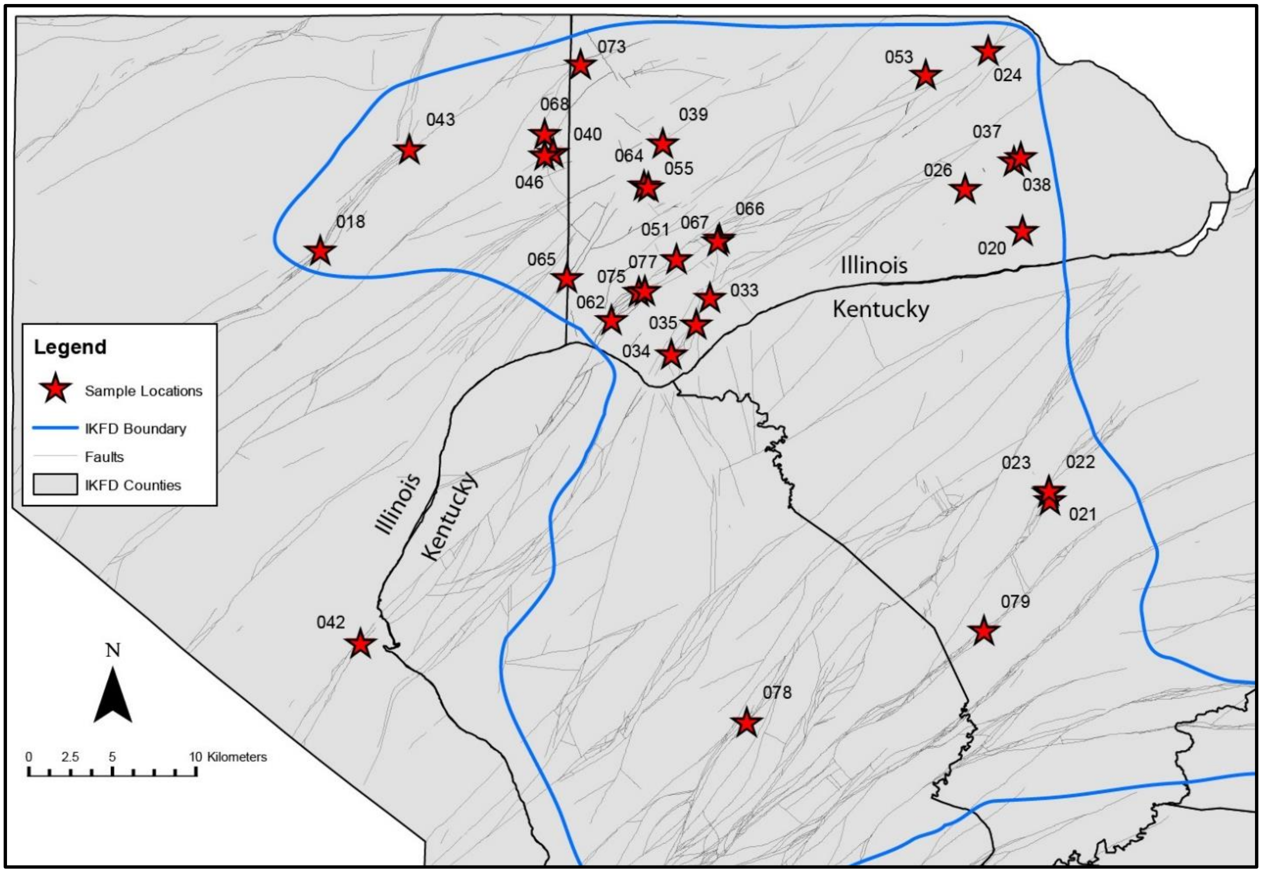

Figure 7. Map showing sample locations analyzed in this study, major structural features of the region, and a boundary of the IKFD.

Table 1. Number and location name of samples analyzed in this study.

Reference No.	*Mine Locality*
018	Clay Diggings Mine
020	Hill Mine
021	Eureka Mine (KY)
022	Columbia Mine
023	Davidson Mine
024	Annabel Lee Mine
026	Hastie Quarry
033	Eureka Mine
034	Fairview Mine
035	Rosiclare Mine
037	East Green Mine
038	North Green Mine
039	Rose Mine
040	Empire Mine
042	Brownsfield Prospect
043	Rock Candy Mine
046	Gullet Prospect
051	Austin Mine
053	Denton Mine
055	Lacey Mine
062	Tri-State Mine
064	Lacey North Prospect
065	Fairbarn Shaft
066	Peckerwood Prospect
067	Montgomery Prospect
068	Connard No. 1
073	Rose Creek Mine
075	Dubois No. 3
077	Dubois Mine
078	Klondike II
079	Davenport Mine

4.2 Analytical Methods

Fluorite chemistry was analyzed using Laser Ablation - Inductively Coupled Plasma - Mass Spectrometry (LA-ICP-MS). Analyses were done at Rensselaer Polytechnic Institute (Troy, NY) using an LA-ICP-MS system consisting of a detachable Photon Machines Analyte 193 ultra-short pulse excimer laser ablation (LA) workstation and a Bruker 820-MS inductively coupled plasma mass spectrometer (ICP-MS).

Based on preliminary data, time, and budget constraints, it was determined that the most effective method for analysis was crushing grains in bulk, sieving the grains, and selecting grain fragments that showed the most variety from each location. Epoxy mounting pucks were drilled with 7 holes, each of which were filled with sorted grains from an individual mine location. The grains were placed in their respective holes such that the most variability in grains would be exposed for analysis.

The pucks were then prepared for analysis by sanding the top surface with 600 grit sandpaper to expose the grain surfaces, followed by 1000 grit sandpaper, and then finish polished with 0.5-micron alumina powder. Two grain mounts could be mounted in the Excimer Laser at the same time. Warm up time with the laser was approximately ½ hour. Chamber gas was always purged with helium when new fluorite samples were inserted into the laser. Fluorite was analyzed using 150-micron square pits at 100% power. The laser fired at 6Hz, or 240 spots over a 40 second period. The mass spectrometer begins gathering data before the laser fires, while the laser is firing, and continues to gather data for an additional 52 seconds, for a total time of 92 seconds per analysis. Calcite samples were analyzed with all of the same settings as fluorite, except the laser power was set to 86% for proper ablation. The NIST glass standard 612 was used for each analysis. The standard was analyzed 4 times before the start of each analytical session, and also analyzed twice every 10 spots in order to determine analytical stability. Ten grain fragments were analyzed from each sample location. Over 530 grain fragments were analyzed from 32 sample locations.

Chapter 5: Results

5.1 Fluorite

For analysis of the data, the REEs are classified as the light REEs (LREE), La through Nd; the medium REEs (MREE); Sm through Ho, and the heavy REEs (HREE), Er through Lu. Y is included after the HREEs due to its [3^+] valance state and similar ionic radii to Ho. REE concentrations are normalized to chondrite values obtained from Taylor and McLennan (1985).

Overall, the data show that REE patterns and concentrations in fluorite samples across the District are similar, but there are subtle, distinct differences, allowing me to identify two separate REE patterns. In general, with the exception of a sample from the Sparks Hill Diatreme, REE patterns in fluorite across the District are characterized by LREE depletion, MREE enrichment, and varying degrees of HREE depletion. All samples have strong positive Y anomalies. REE concentrations for all elements, except Y, do not exceed 100x chondrite (10ppm) for any location sampled besides the Sparks Hill Diatreme.

In detail, there are two distinct REE patterns that commonly appear in fluorite. The first pattern, is found at sample locations throughout the District including 020, 022, 024, 026, 033, 037, 038, 053, 065, and 067 (Figs. 8A, B, C, E, and J; see Table 1 for mine names). This pattern is characterized by LREE depletion, no positive Eu anomaly, a maximum at Gd, sometimes showing a positive Gd anomaly, and gently negative sloping HREEs. A less distinct version of the first pattern appears in Hicks Dome samples 039, 055, and 064, of which 064 has the highest REE concentrations and least LREE depletion (Fig. 8D). The second REE pattern, most notable in samples 020, 034, 040, 051, 062, 073, 075, and 077 (Figs. 8F, G, H, and I), is made up of LREE depletion similar to that of the first pattern, and a maximum at Eu with some samples showing a distinct positive Eu anomaly. The Gd:Lu ratios of the second pattern are on average slightly higher than the first pattern.

There seems to be no correlation between REE pattern and overall REE concentration; however, there is a slight decrease in total REE concentration away from Hicks Dome towards the fringes of the District, with the most notable exception of fluorite from location 037, the East Green Mine, which showed anomalously high MREE and HREE concentrations relative to nearby samples. At no location sampled throughout the District was primary fluorite found to occur with LREE enrichment or high concentrations of REEs that could be indicative of intergrown REE-bearing mineral phases.

In addition to the rare earth elements, fluorite was analyzed for Al, Cu, Zn, Pb, Sr, Ba, Th, and U concentrations. At some locations there is a correlation between paragenetically early fluorite and higher overall concentrations of Sr; however, no other trace element concentrations are distinguishable between known early and late fluorite.

Illinois Samples

A 024 Annabel Lee Mine

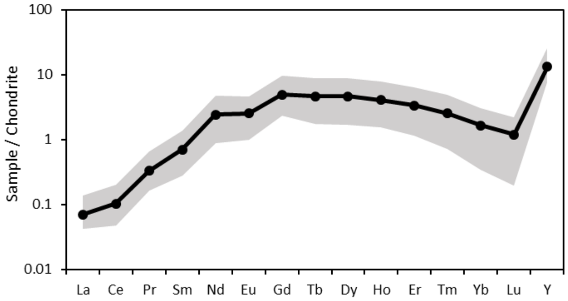

B 026 Hastie Quarry

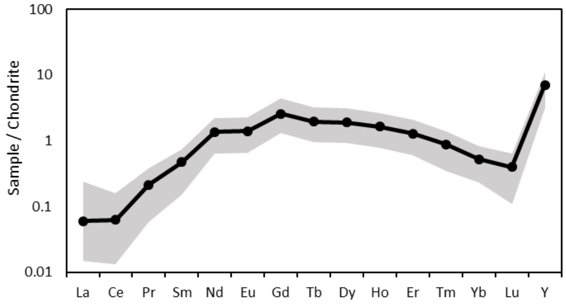

C 037 East Green Mine

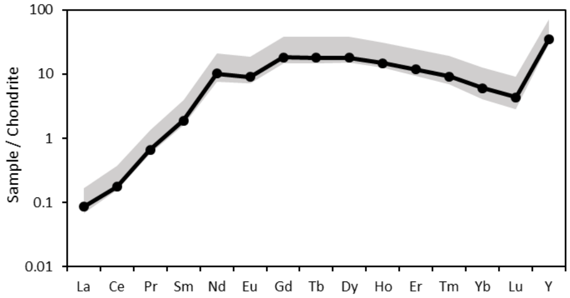

D 064 Lacey North Prospect

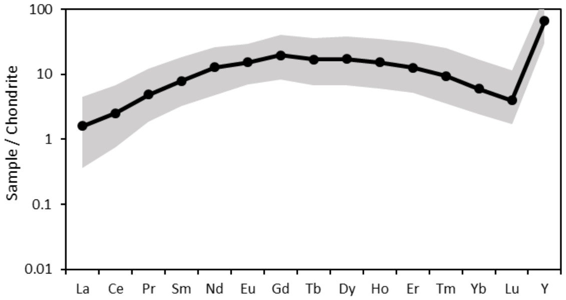

F 040 Empire Mine

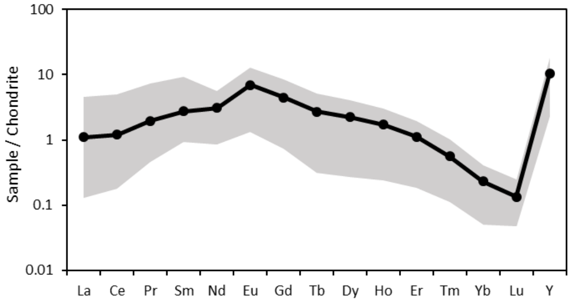

G 062 Tristate Mine

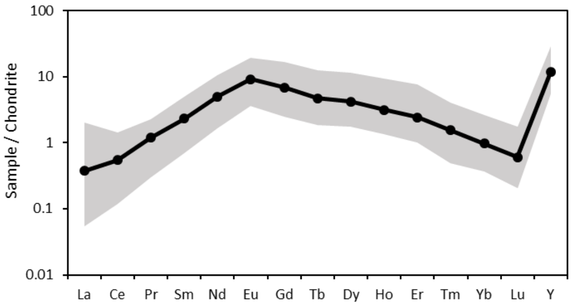

H 073 Rose Creek Mine

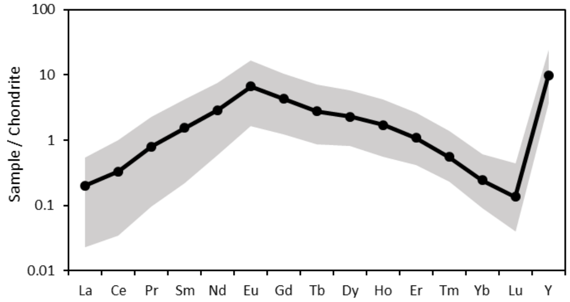

I 077 Dubois Mine

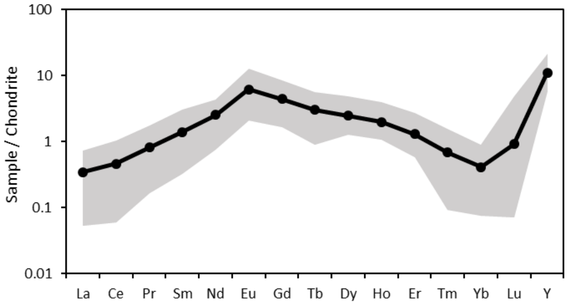

Kentucky Samples

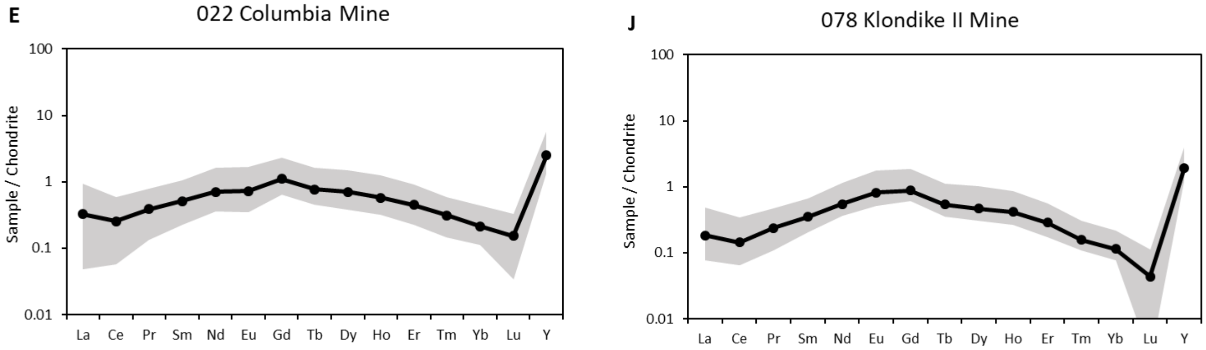

Figure 8. Average chondrite normalized REE patterns of selected locations throughout the District which have similar grain-to-grain REE patterns. Grey areas represent the range of values and data lines represent the mean value for each element based on 5-10 analyses. Concentrations normalized to chondrite values from Taylor and McLennan (1985).

REE patterns of fluorite from the Sparks Hill Diatreme are similar to the REE pattern of the diatreme itself and of other intrusive rocks throughout the District (Denny et al., 2015) (Figs. 9 and 29). This fluorite is enriched in LREEs and shows negative sloping MREEs and HREEs, with a positive Gd anomaly (Fig. 9). The Gd anomaly is also present in the whole rock data for the diatreme. Y/Ho ratios for this sample are equivalent, to slightly lower, compared to fluorite sampled across the District. REE concentrations in the sample, unlike the regional intrusive rocks however, do not exceed 1000x chondrite for any of the REEs.

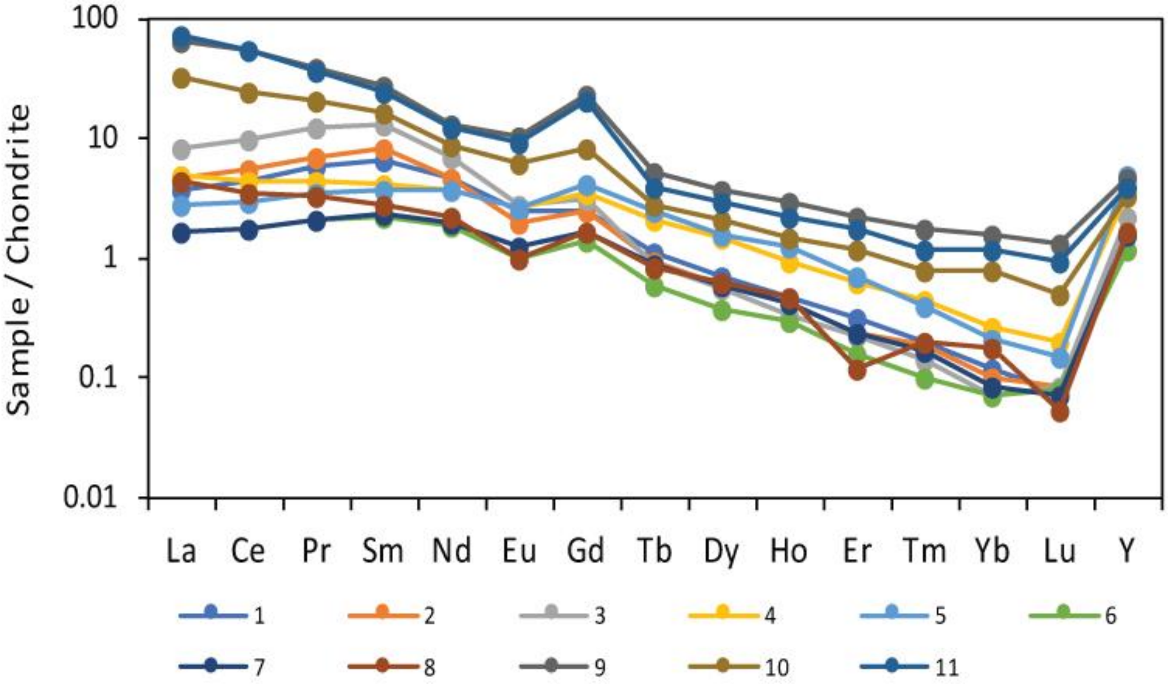

Figure 9. Chondrite normalized REE patterns of secondary fluorite within the Sparks Hill Diatreme. Concentrations normalized to chondrite values from Taylor and McLennan (1985).

5.2 Calcite

REE concentrations from ore-stage calcite samples from many locations were higher overall compared to fluorite samples from the same mine. Many calcite samples show flatter REE patterns than fluorite from their respective mines, and several samples showed distinct positive Eu anomalies. Positive Y anomalies are present in several calcite samples; however, Y/Ho ratios are much lower compared to those in fluorite samples from the same mine. Calcite samples showed much greater incorporations of Sr compared to fluorite from the same location. Overall, REE data in calcite was not systematic and with a lack of data from other districts to compare to, REE patterns in calcite were not found to be useful in this study.

Chapter 6: Discussion

Fluorite occurs throughout the world in sedimentary, igneous, and metamorphic rocks and can form from a variety of hydrothermal fluids, and the REE geochemistry of fluorite has been proven valuable in helping determine the source and characteristics of hydrothermal mineralizing fluids (e.g., Bau et al., 2003; Schwinn and Markl, 2005; Ehya et al., 2010). Fluorite is an excellent mineral for the study of the chemistry and chemical evolution of hydrothermal fluids because of the similar chemical behavior of the REEs and their non-selective partitioning into fluorite with cubic crystal habits (Bosze and Rakovan, 2001), which is the predominant crystal habit of IKFD fluorite. The REE patterns of fluorite, as well as their concentrations, can be indicative of associated REE mineral deposits; for example, fluorite with anomalously high concentrations of REE (over 1000x chondrite) in the Hick Dome diatreme is associated with REE-enriched minerals, as described above.

6.1 Evidence for a Regional Thermal Gradient in Mineralizing Fluids

Fluid inclusion and geochemical data in the IKFD indicate that the carbonatite intrusion below Hicks Dome acted as a source of heat (Taylor et al., 1992) and REEs (Burruss et al., 1992) for regional mineralizing fluids, resulting in a regional thermal gradient. Additional evidence for magmatic heat at Hicks Dome includes outcrops of slate rather than the Devonian New Albany shale in the core of the Dome. Since previous studies indicate that Hicks Dome was a thermal "hot spot" and that regional temperature decreased away from the Dome, fluorite sample locations can be arranged according to their distance from Hicks Dome to explore whether any REE or trace element trends can be explained by a regional thermal gradient, or alternatively, by a chemical gradient away from Hicks Dome, perhaps coupled to variation in fluid temperature. Average elemental concentrations are used for each sample location to show the general trend in REE and trace element behavior on a region-wide scale, and aside from the slight differences in paragenetically early and later fluorite, in general, we found only small grain-to-grain variations and very low analytical error (Table 2), thus making average sample location compositions useful.

There is an overall decrease in the average concentration of LREEs, MREEs, and HREEs away from Hicks Dome, (Fig. 10). Average Y concentration also decreases away from Hicks Dome (Fig. 11), and while the average Y/Ho ratio is variable, the ratio stays fairly consistent to the fringes of the District (Fig. 12). Although Y is similar in size and charge to the other [3^+] REEs in hydrothermal fluids, it has been shown to have unique behaviors in hydrothermal fluids. At high fluoride activities, presumably as in mineralizing fluids across the IKFD, Y does not form mono-fluoride complexes ($REEF^{2+}$) like the other REEs (Migdisov et al., 2009), but instead forms di-fluoride complexes (YF_2^+) at temperatures of 100–250°C (Loges et al., 2013). The formation of di-fluoride complexes allows for the preferential partitioning of Y into fluorite relative to Ho (Loges et al., 2013) and could explain the large positive Y anomaly that is found in IKFD and in other sedimentary brine-related fluorites (Bau et al., 2003; Mao et al., 2016).

Samples 053, 026, 024, 037, and 038 have elevated concentrations of Sr compared to other sample locations at similar distances from Hicks Dome (Fig. 13). A possible explanation for variation in Sr could be that these five sample locations are found within the Harris Creek and Cave-in-Rock subdistricts, known for their large bedding replacement deposits (Fig. 3). Large amounts of carbonate dissolution are required for the formation of bedding replacement deposits and this could have resulted in an increase of dissolved Sr from calcite and dolomite into the mineralizing fluids, which was later re-incorporated into fluorite. A seemingly random arrangment of mines away from Hicks Dome also have high average concentrations of either Ba or Th (Figs.

14 and 15) and there seems to be no correlation between these trace element anomalies and high average concentrations of REEs from the same fluorite samples, nor any systematic correlation that could be explained by a regional temperature gradient. Th is the most perplexing trace element as the highest concentrations of Th would be excepcted to occur in close proximity to Hicks Dome due to the elevated Th concentrations in intrusive rocks at Hicks Dome.

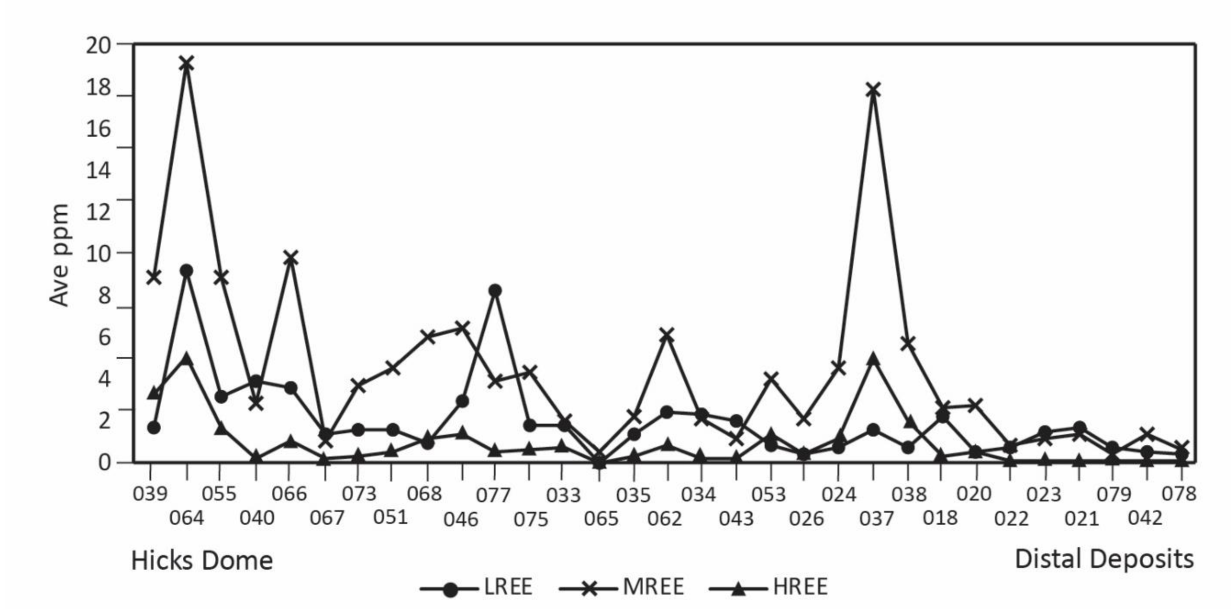

Figure 10. Average light, medium, and heavy REE concentrations in order of increasing distance from Hicks Dome.

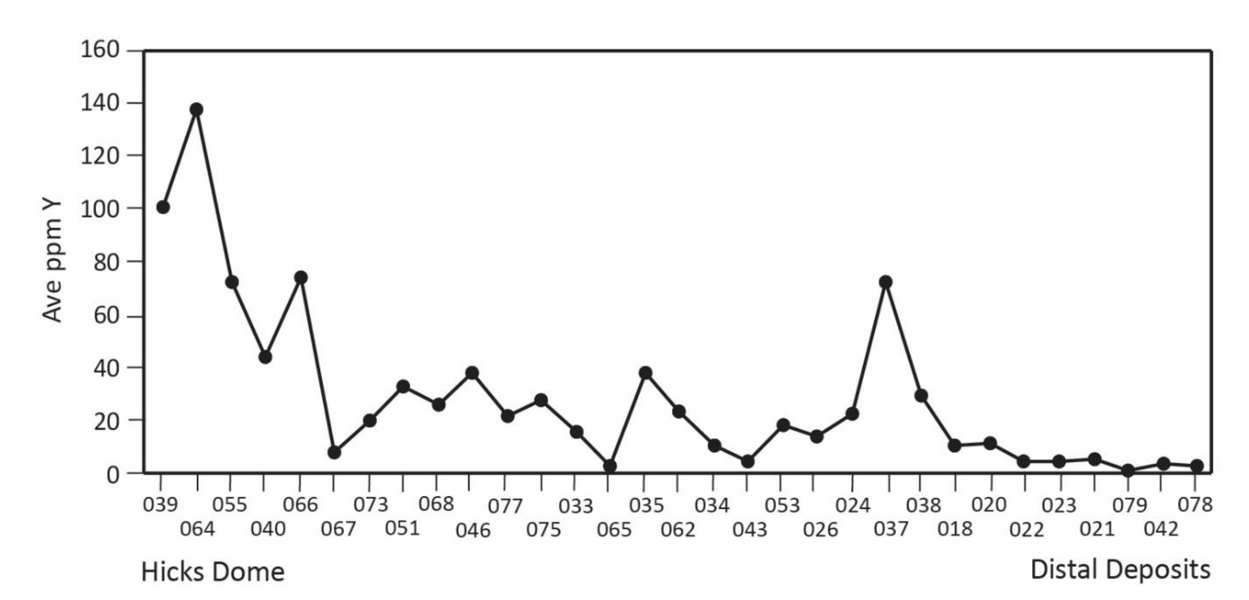

Figure 11. Average yttrium concentration in order of increasing distance from Hicks Dome.

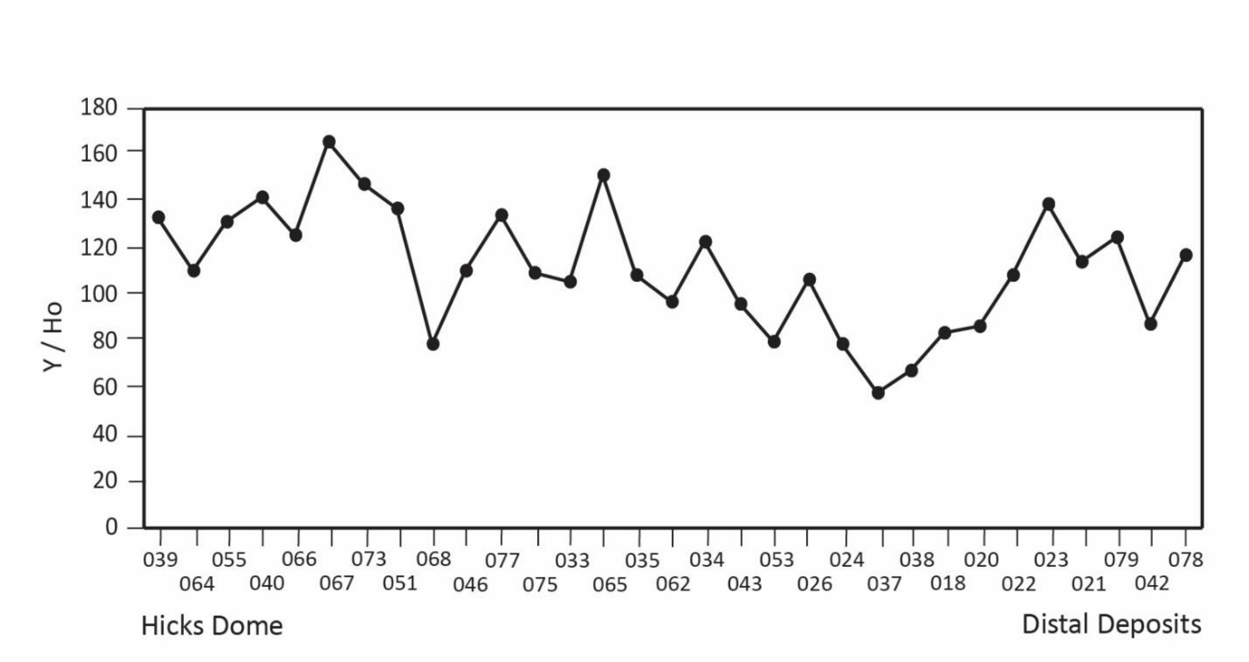

Figure 12. Average yttrium / holmium ratio in order of increasing distance from Hicks Dome.

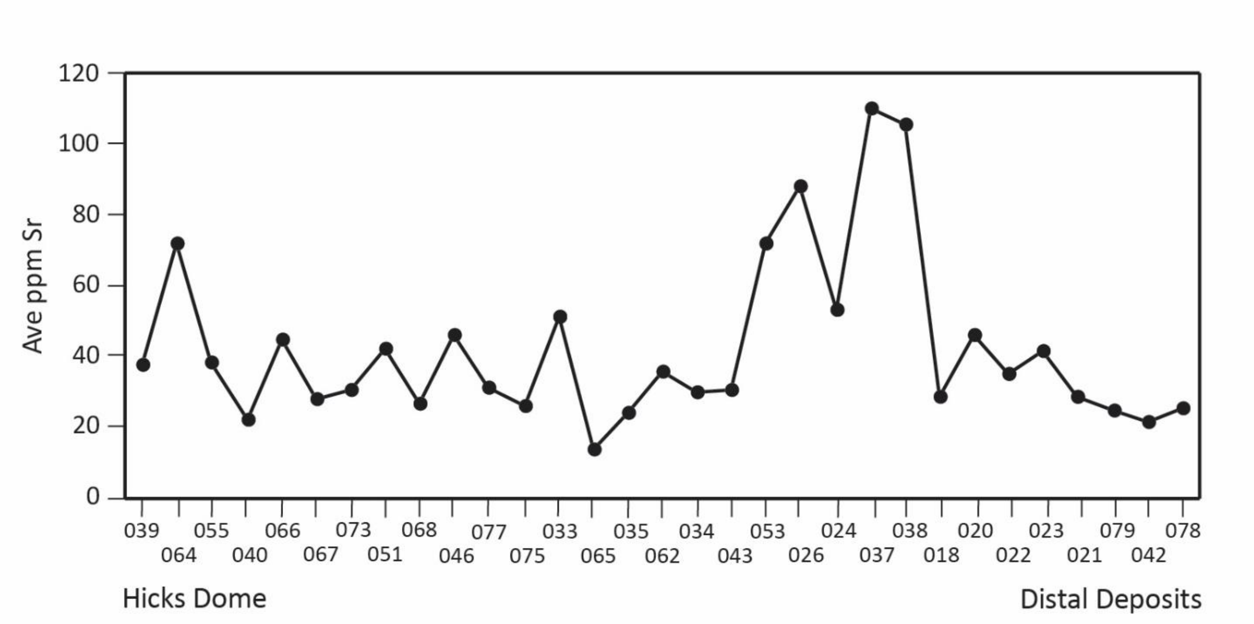

Figure 13. Average strontium concentration in order of increasing distance from Hicks Dome.

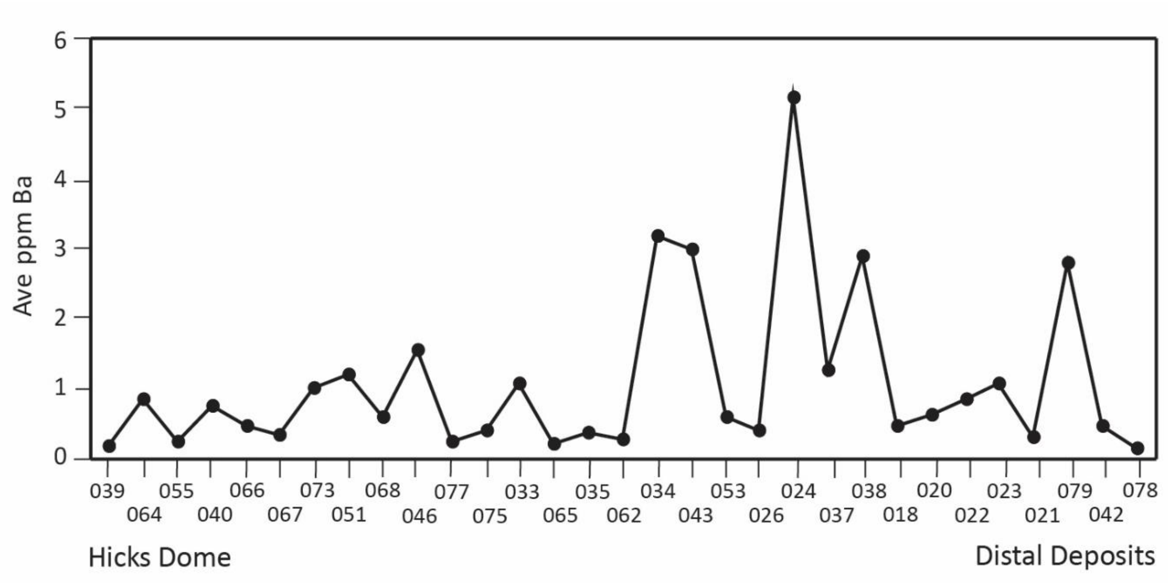

Figure 14. Average barium concentration in order of increasing distance from Hicks Dome.

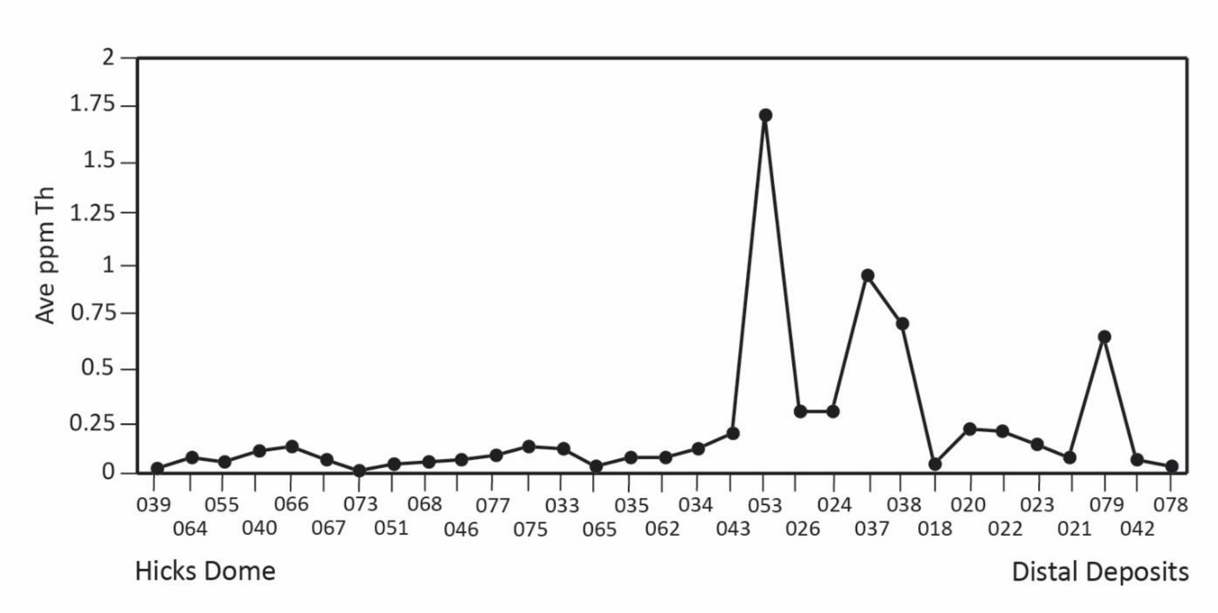

Figure 15. Average thorium concentration in order of increasing distance from Hicks Dome.

The Clay Diggings Mine (018) and the Brownsfield Prospect (042) are two sample locations at the furthest western extent of the District in Illinois (Fig. 7). Both locations have at least one chemical anomaly that is characterized by LREE enrichment and comparatively lower concentrations of MREEs and HREEs (Fig. 16 Analysis 3, 4, and 6; Fig 17 Analysis 8). Based on high concentrations of lead, zinc, and/or aluminum in fluorite from both locations these anomalies appear to be caused by the ablation of inclusions trapped within the fluorite crystals. Fluorite from these two locations have similar REE patterns, with Clay Diggings Mine fluorite containing higher REE concentrations compared to Brownsfield Prospect fluorite (Figs. 16 and 17). The higher REE concentrations in Clay Diggings Mine fluorite could be the result of Clay Diggins being closer to Hicks Dome. Neither location shows a positive Eu anomaly and although they lack a significantly positive Gd anomaly, they both appear to be slight variations of the early F1 fluorite REE pattern; however, the location of the samples within the paragenetic sequence is not known at these locations.

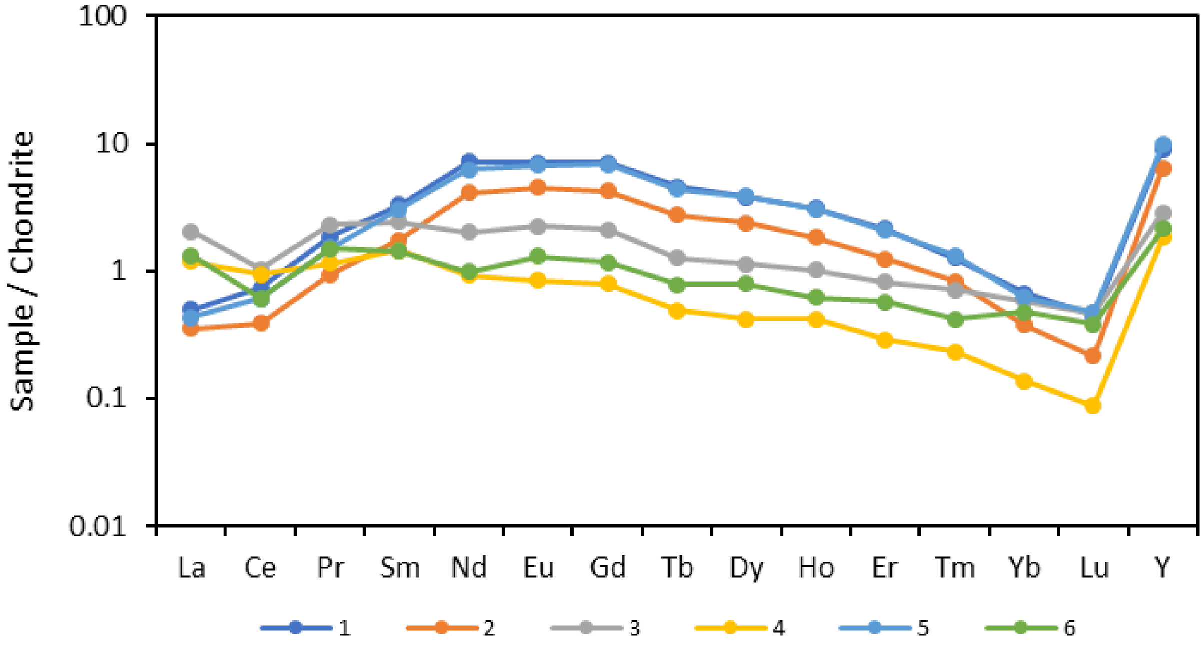

Figure 16. Chondrite normalized REE patterns of fluorite from the Clay Diggings Mine (018). Fluorites 3 and 6 contain high lead and zinc concentrations, while fluorite 4 contains no anomalous concentrations of any non-REE trace elements analyzed.

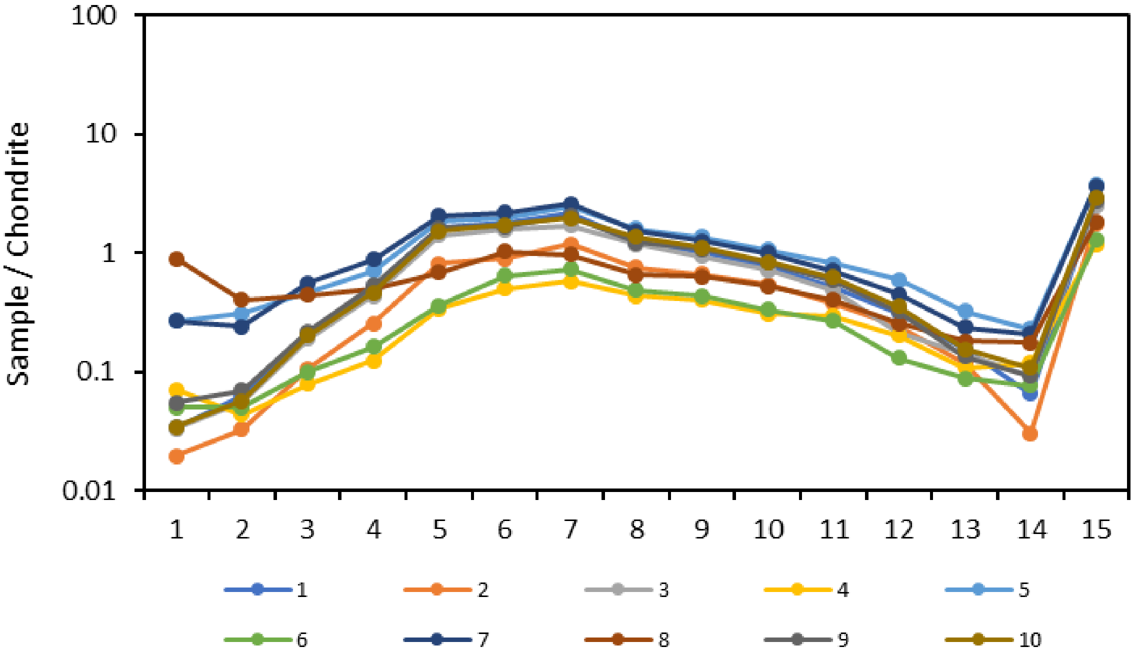

Figure 17. Chondrite normalized REE patterns of fluorite from the Brownsfield Prospect (042). Fluorite 8 contains high aluminum, lead, and zinc concentrations.

The Kentucky fluorite samples have similar concentrations of LREEs compared to samples from the rest of the District, but lower concentrations of MREEs and HREEs and overall flatter patterns (Fig. 8E and 8J). This could be a reflection of mineralizing fluids that reached sites of ore deposition farther away from sources of magmatic heat underlying the District. REE-fluoride complexes have been believed to be one the primary transport species of REEs in fluorine-rich solutions in addition to REE-chloride complexes (Sheard et al., 2012). Although recent modelling by Migdisov and Williams-Jones (2014) suggests that the REEs are transported predominantly as REE-chloride complexes in acidic, fluorine-rich solutions, much of the previous body of work on REE transport in solution focuses on the behavior of REE-fluoride complexes. LREE-fluoride and LREE-chloride complexes have been shown to dissociate less readily than HREE complexes

(Sheard et al., 2012) and LREE-fluoride complexes have been found to be more stable at higher temperatures than HREE-fluoride complexes (Migdisov et al. 2009). Richardson and Holland (1979) determined that fluorine solubility decreases with decreasing temperatures. Decreasing fluid temperatures and subsequent decreasing fluorine concentrations in the mineralizing fluids could have resulted in the preferred destabilization of MREE- and HREE-fluoride complexes over LREE-fluoride complexes. This would result in decreased MREEs and HREEs in fluorite at the fringes of the District, which could also explain the flattened REE patterns seen at these locations. In summary, decreases in Y and REEs in fluorite could be explained by a decrease in temperature of fluorite mineralizing fluids with increasing distance from Hicks Dome.

6.2 REE Patterns and Two Mineralizing Fluids

As discussed previously, the chondrite normalized data shows the occurrence of two primary REE patterns in many of the samples. The REE patterns of known paragenetically early fluorite samples (yellow 1 through purple 3, Fig. 4) from this study should be indicative of fluorite formed from the lower temperature-higher salinity (F1) fluid that Spry et al. (1990) found in paragenetically early fluorite within the Denton mine and that Spry and Fuhrmann (1994) found in the Annabel Lee, Minerva, and Hill mines. The second REE pattern, characterized by a positive Eu anomaly, should then be indicative of fluorite formed later in the paragenetic sequence (blue 1 through purple 6, Fig. 4) from a higher temperature-lower salinity mineralizing (F2) fluid (Spry and Fuhrmann, 1994). My REE data show that paragenetically early F1 fluorite can be distinguished from later F2 fluorite by their respective REE patterns at many locations throughout the District.

Fluorite samples analyzed from the Hill Mine (020) clearly show both REE patterns (Fig. 18). In addition, early F1 fluorite from the Hill Mine has higher overall concentrations of Sr and Th compared to later F2 fluorite. At the Hill Mine, early F1 fluorite contains higher concentrations of MREEs and HREEs than later F2 fluorite, which seems counterintuitive to early fluorite forming from a lower temperature F1 fluid in which REEs are less stable in solution. However, if F1 fluids migrated through the Ordovician St. Peter Sandstone, the fluids may have incorporated higher concentrations of MREEs and HREEs due to fluid-rock interactions with the REE-bearing Ordovician phosphorites that are present within the Illinois basin (Emsbo et al., 2015).

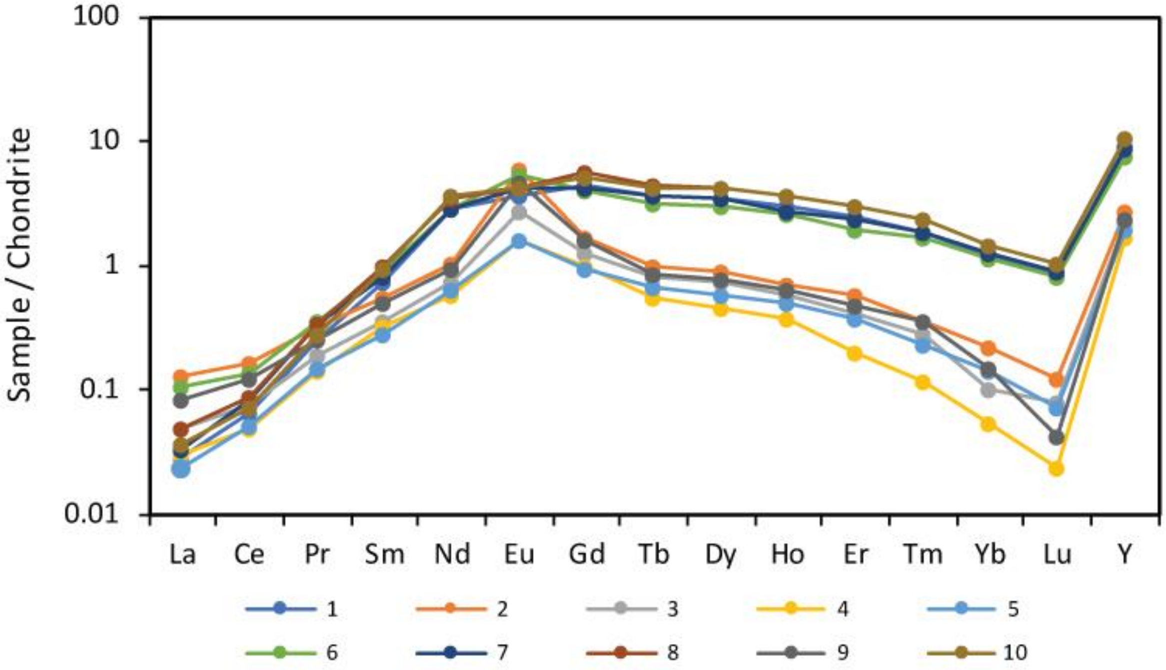

Figure 18. Chondrite normalized REE patterns of fluorite from the Hill Mine (020). Fluorites 6, 7, 8, and 10 comprise the early F1 fluorite pattern while fluorites 1, 2, 3, 4, 5, and 9 make up the late F2 fluorite pattern.

Table 2. Sample data table for the Hill Mine (020). The complete data set for this study can be found at UC Scholar (http://dx.doi.org/doi:10.7945/C2438P).

	La (ppm)	**La (error)**	**Ce (ppm)**	**Ce (error)**	**Pr (ppm)**	**Pr (error)**	**Nd (ppm)**	**Nd (error)**	**Sm (ppm)**	**Sm (error)**
Sample 1	0.0108	0.0016	0.0619	0.0039	0.0357	0.0024	0.521	0.022	0.667	0.033
Sample 2	0.0478	0.0032	0.1556	0.0071	0.0444	0.0025	0.392	0.024	0.241	0.022
Sample 3	0.0181	0.0019	0.0723	0.0038	0.0256	0.0022	0.254	0.022	0.172	0.014
Sample 4	0.011	0.0017	0.0472	0.004	0.02	0.002	0.231	0.018	0.134	0.014
Sample 5	0.0088	0.0012	0.0505	0.0046	0.0204	0.0021	0.2	0.015	0.15	0.013
Sample 6	0.0389	0.0044	0.133	0.011	0.0497	0.0034	0.624	0.038	0.647	0.037
Sample 7	0.0122	0.002	0.0813	0.0067	0.0457	0.0041	0.589	0.036	0.661	0.038
Sample 8	0.0179	0.0031	0.0858	0.0079	0.047	0.0042	0.711	0.044	0.816	0.058
Sample 9	0.0313	0.0037	0.1175	0.0079	0.0354	0.0041	0.349	0.029	0.22	0.027
Sample 10	0.0136	0.0026	0.068	0.0054	0.0389	0.0035	0.655	0.042	0.84	0.057

	Eu (ppm)	**Eu (error)**	**Gd (ppm)**	**Gd (error)**	**Tb (ppm)**	**Tb (error)**	**Dy (ppm)**	**Dy (error)**	**Ho (ppm)**	**Ho (error)**
Sample 1	0.32	0.014	1.356	0.062	0.2106	0.0096	1.304	0.061	0.2509	0.0099
Sample 2	0.514	0.021	0.521	0.032	0.0582	0.0042	0.349	0.026	0.0613	0.0048
Sample 3	0.234	0.012	0.378	0.025	0.0478	0.0026	0.276	0.02	0.0491	0.0035
Sample 4	0.1383	0.0082	0.309	0.028	0.0319	0.0028	0.171	0.017	0.0317	0.0034
Sample 5	0.1393	0.0093	0.29	0.02	0.0389	0.0031	0.224	0.014	0.043	0.0032
Sample 6	0.46	0.021	1.201	0.055	0.179	0.0088	1.135	0.058	0.223	0.011
Sample 7	0.372	0.019	1.307	0.064	0.207	0.011	1.295	0.069	0.229	0.013
Sample 8	0.366	0.022	1.698	0.098	0.257	0.014	1.6	0.089	0.309	0.016
Sample 9	0.409	0.029	0.482	0.04	0.0505	0.0051	0.294	0.026	0.0532	0.0057
Sample 10	0.375	0.024	1.602	0.098	0.24	0.012	1.604	0.084	0.31	0.016

	Er (ppm)	**Er (error)**	**Tm (ppm)**	**Tm (error)**	**Yb(ppm)**	**Yb (error)**	**Lu (ppm)**	**Lu (error)**	**Y (ppm)**	**Y (error)**
Sample 1	0.605	0.032	0.0667	0.0042	0.299	0.022	0.033	0.0036	19.14	0.6
Sample 2	0.143	0.012	0.0128	0.0019	0.0538	0.0083	0.0046	0.0018	5.6	0.21
Sample 3	0.1018	0.0087	0.0102	0.0016	0.0257	0.0055	0.003	0.0012	4.67	0.15
Sample 4	0.0505	0.0064	0.0043	0.0012	0.0137	0.0047	0.0009	0.0012	3.59	0.13
Sample 5	0.0927	0.0084	0.0085	0.0013	0.0359	0.0063	0.0028	0.0013	4.14	0.14
Sample 6	0.496	0.03	0.0594	0.0038	0.29	0.02	0.0305	0.0035	16.17	0.57
Sample 7	0.595	0.032	0.0682	0.005	0.318	0.025	0.0347	0.0038	18.65	0.64
Sample 8	0.753	0.036	0.0845	0.0071	0.367	0.035	0.0389	0.0049	22.49	0.83
Sample 9	0.119	0.013	0.0128	0.0023	0.0374	0.0097	0.0016	0.0024	4.86	0.19
Sample 10	0.764	0.045	0.0858	0.0062	0.367	0.028	0.0385	0.0045	22.24	0.81

6.3 Anomalous REE Patterns

Multiple re-analyses of samples from the Montgomery Prospect (067) yielded the typical pattern found in early F1 fluorite, in addition to an anomalous pattern that has no link to fluid or mineral inclusions within the grains and thus appears to be an accurate reflection of the REE pattern of those grains (Fig. 19). This anomalous pattern shows higher concentrations of LREEs, but also with a positive slope, a maximum at Sm, and lower concentrations of MREEs and HREES than other fluorite samples from the Montgomery Prospect. From Eu through Lu, although lower in concentration, the anomalous REE pattern is strikingly similar to the early F1 fluorite REE pattern. This anomalous pattern could be a reflection of fluid variation from localized fluid-rock interactions at the site of ore deposition, and further analysis will be needed to explain this anomaly.

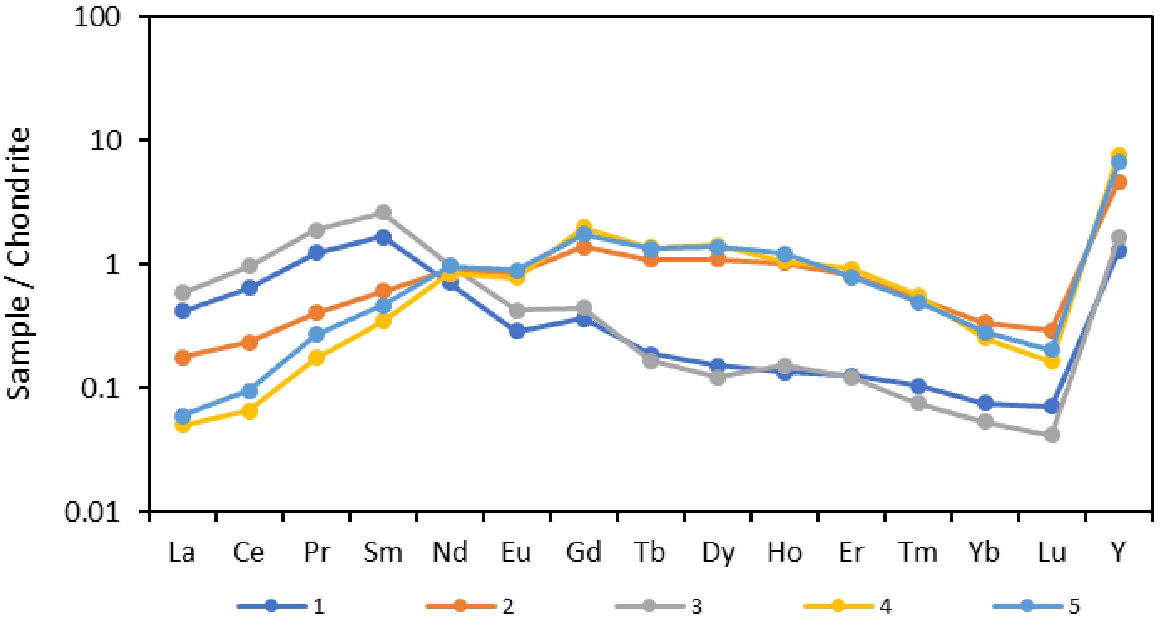

Figure 19. Chondrite normalized REE patterns of fluorite from the Montgomery Prospect (067). Fluorites 2, 4, and 5 comprise the early F1 fluorite pattern while fluorites 1 and 3 make up an anomalous pattern.

Additional analysis of fluorite grains from the Rose Mine (039) (Fig. 20) returned several similar patterns (Fig. 20; fluorites 1 through 8); however, several grains showed anomalously low concentrations of REEs, less than 1x chondrite for all elements with the exception of Y (Fig. 20;

fluorites 9 through 13). The anomalous patterns are much flatter overall, but still show a maximum at Gd, have strong positive Y anomalies, and these grains have very similar trace element concentrations to fluorites 1 through 8 from the Rose Mine. The anomalous patterns most closely resemble the REE patterns from sample locations furthest away from Hicks Dome (Fig. 8E and 8J). However, further analysis will be needed to determine the cause of the significant variation within samples from the Rose Mine and if the low REE samples correspond to the clear zone between purple 6 and purple 7 as noted by Burruss et al. (1992) to be depleted in REEs.

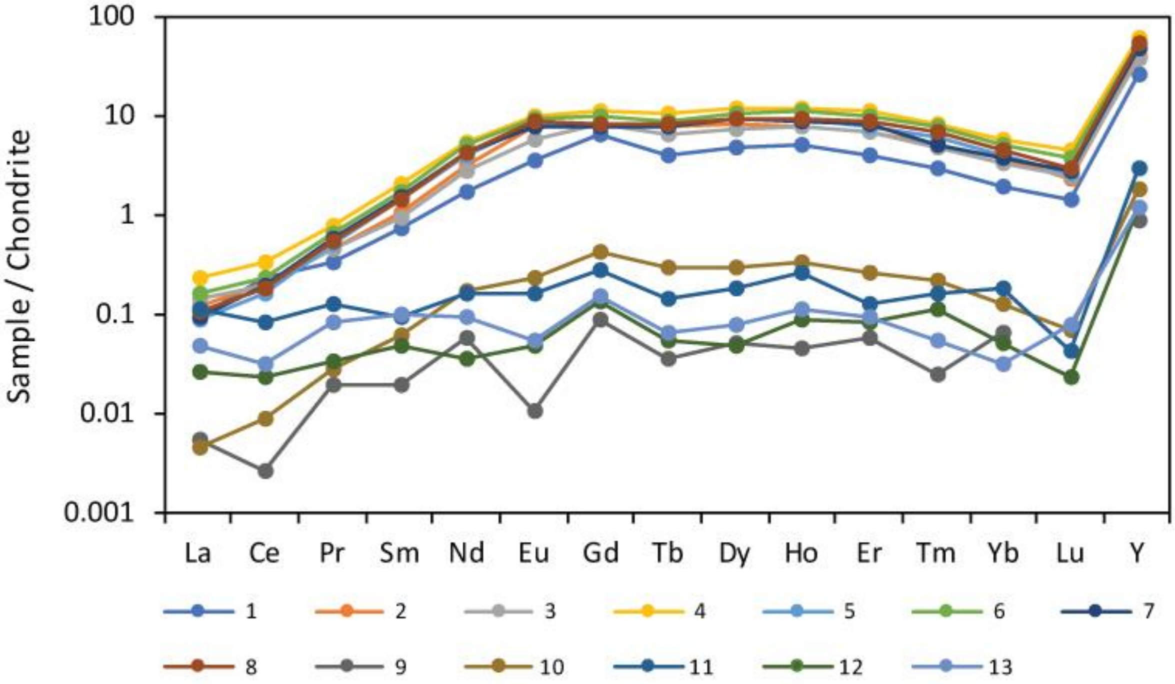

Figure 20. Chondrite normalized REE patterns of fluorite from the Rose Mine (039).

6.4 Comparison to Previous REE Analyses in the IKFD

Over 25 years ago, Burruss et al. (1992) looked at the regional zonation of REEs in fluorite across the IKFD using instrumental neutron activation, in addition to microscale zonation analysis with LA-ICP-MS and laser excited photoluminescence spectroscopy. The authors noted that purple fluorite from the Rose Mine contained the highest total REE concentrations and was the only sample analyzed to be enriched in both MREEs and HREEs. The authors found that early fluorite (yellow 2 and purple 2, Fig. 4) contained the highest total REE concentrations from individual mines, and later fluorite had either decreasing or fluctuating REE content. They determined that a clear fluorite zone separating the purple 6 and purple 7 zones was considerably lower in total REEs and contained abundant hydrocarbon inclusions. This paper was published in an USGS Open File Report and no REE graphs or data tables are available with it.

The Rose Mine occurs at the top of Hicks Dome in a mineralized breccia body. Hicks Dome is one of the few locations throughout the District where green fluorite is common; it is found in fluorite from the Rose Mine breccia and was reported by Brown et al. (1954) to be common in veinlets of the uppermost (310–330 ft) section of the Henry Hamp, Jr. No. 1 well above the large mineralized Hicks Dome breccia. Light green, clear, and minor purple fluorite were analyzed from the Rose Mine repeatedly as part of my study, and unlike the findings of Burruss et al. (1992), all colors returned similar REE patterns (Fig. 20, fluorites 1 through 8), with the exception of several clear grains that produced the anomalous patterns (Fig. 20, fluorites 9 through 13). Samples from the Rose Mine do show some of the lowest degrees of HREE depletion out of all locations sampled.

Chesley et al. (1994) analyzed fluorite samples from the Cave-in-Rock and Harris Creek subdistricts located in horsts on either side of the Rock Creek Graben to the east of Hicks Dome (Fig. 3). The authors prepared samples by crushing grains, dissolving them in a combination of $HCLO_4$ and HNO_3, drying them, re-dissolving them in HNO_3, and drying them again. The samples were analyzed for REE abundances using ICP-MS and the authors analyzed samples of known location within the paragenetic sequence. Their results for the Hill Mine (020 in this study) differ from those presented here; Chesley and other's patterns show distinct positive Eu anomalies occurring in both early yellow 2 and purple 3, and late purple 6 fluorite (Fig. 21), in addition to patterns with no positive Eu anomaly occurring in early yellow 2 and purple 3 fluorite grains that are more characteristic of early F1 fluorite REE patterns from this study (compare Figs. 18 and 21). The authors' results for early yellow 2 and purple 3 fluorite from the Denton, Annabel Lee, and Minerva mines show patterns with no positive Eu anomaly (Fig. 22, samples DMK44, DMK3A, CR8612, and 70P7A) similar to results in this study. However, clear fluorite bands from purple 3 samples and purple 4 fluorite from the Deardorff Mine returned patterns with positive Eu anomalies (Fig. 22, samples 62P121 and 62P88A). The positive Eu anomaly in the clear bands of purple 3 fluorite could be indicative of the initial influx of F2 fluids into the Mississippian carbonates. Spry and Fuhrmann (1994) found the change in mineralizing fluids to occur at the purple 3 fluorite and purple 4 fluorite boundary, however, this does not explain the occurrence of positive Eu anomalies in early fluorite samples from the Hill Mine. Chesley and other's results also show negative Ce anomalies and higher concentrations of La compared to results obtained in this study.

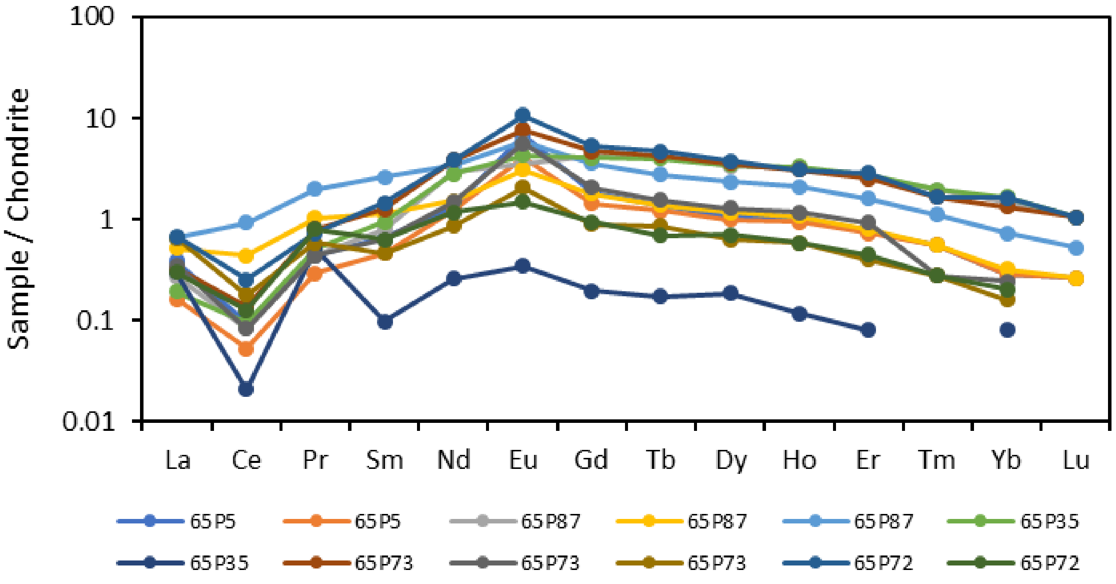

Figure 21. REE patterns of fluorite from the Hill Mine, from Chesley et al. (1994), normalized to chondrite values from Taylor and McLennan (1985).

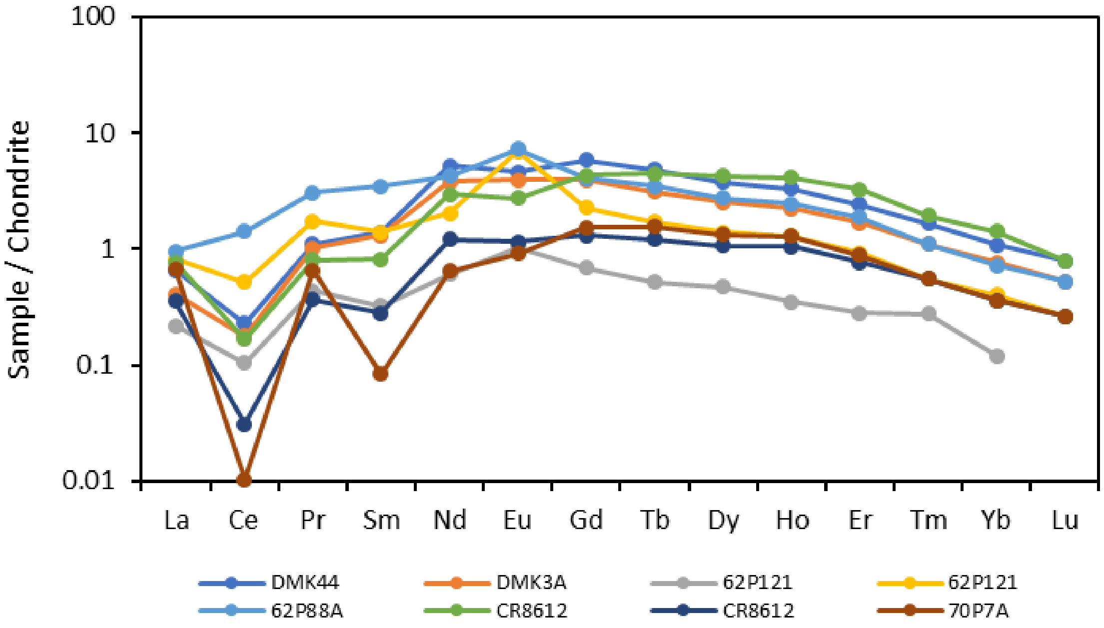

Figure 22. REE patterns of fluorite from the Denton, Deardorff, Annabel Lee, and Minerva Mines, from Chesley et al. (1994), normalized to chondrite values from Taylor and McLennan (1985).

Mao et al. (2016) analyzed fluorite from the Hastie Quarry (026 in this study) and the Barnett Mine (not sampled in this study), using LA-ICP-MS. Their analysis of fluorite from the Hastie Quarry returned both REE patterns and concentrations identical to those obtained in this study, with fluorite characterized by the distinct early F1 REE pattern. Chondrite normalized REEs in Barnett Mine fluorite were of similar concentration and pattern to F2 fluorite from the rest of the District, marked by the distinct, positive Eu anomaly (Fig. 23).

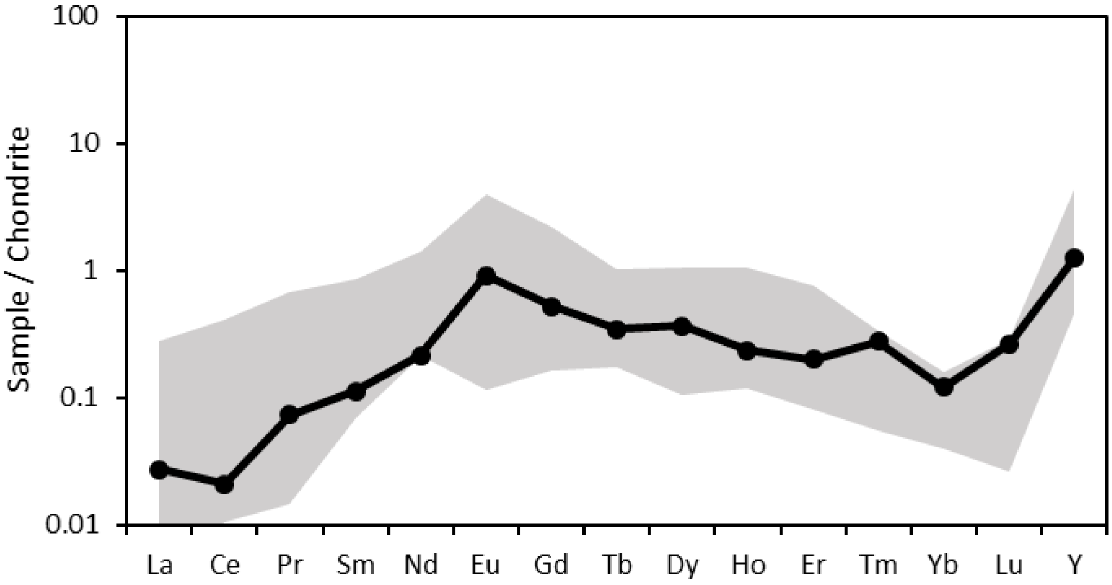

Figure 23. REE patterns of fluorite from the Barnett Mine, from Mao et al. (2016), normalized to chondrite values from Taylor and McLennan (1985). The grey area represents the range of values and the data line represents the median value for each element.

6.5 Insights from Other Fluoritic MVT Deposits

6.5.1 Central Tennessee District

Mao et al. (2016) also analyzed fluorite from the Gordonsville and Elmwood Mines, which are two major mines from the Central Tennessee MVT District (Fig. 5). The Central Tennessee

District is primarily made up of calcite, sphalerite, galena, fluorite, and barite mineralization within lower Ordovician dolostones, with main stage ore fluid temperatures ranging from 97–133°C and fluid salinities of 21–23 weight % NaCl equivalent (Gratz and Misra, 1987). Chondrite normalized REE patterns in Central Tennessee fluorite are characterized by concave-downward patterns with MREE enrichment and positively sloping LREEs and negative sloping HREEs (Mao et al., 2016) (Figs. 24 and 25). Fluorite from both mines shows a slight maximum at Eu, and MREE concentrations are similar to fluorite from the fringes of the IKFD. Unlike the IKFD, fluorite from these two Tennessee mines has more gently positive LREE slopes. This could be due to mineralizing fluids from the Central Tennessee District and the IKFD originating from different source basins and sediments. The occurrence of a positive Tm anomaly from both locations in Central Tennessee could be due to a noisy signal during ablation.

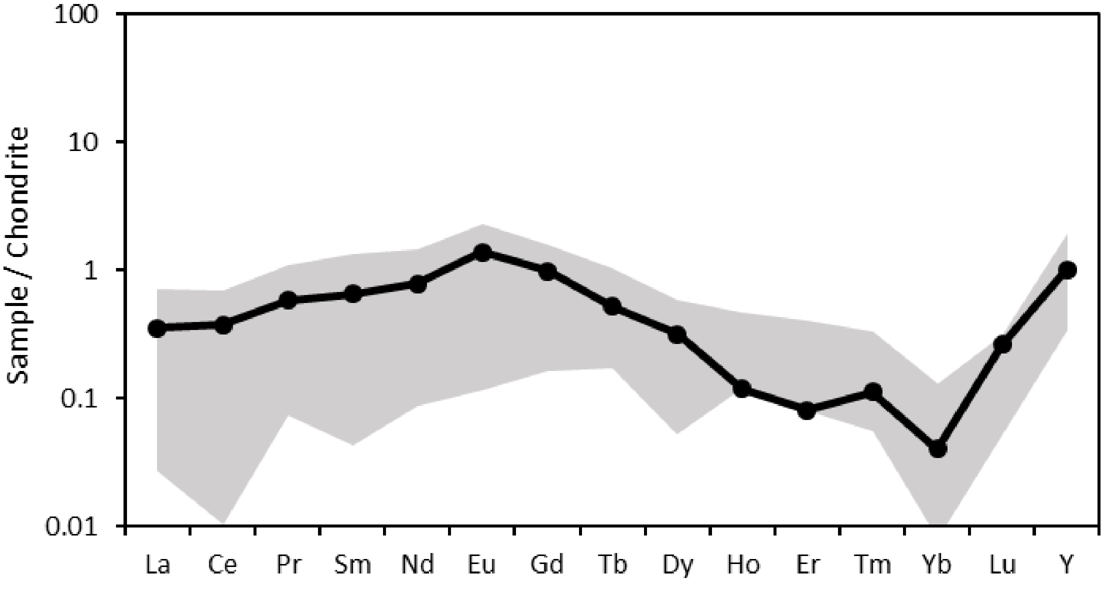

Figure 24. REE patterns of fluorite from the Elmwood Mine, Tennessee, from Mao et al. (2016), normalized to chondrite values from Taylor and McLennan (1985). The grey area represents the range of values and the data line represents the median value for each element.

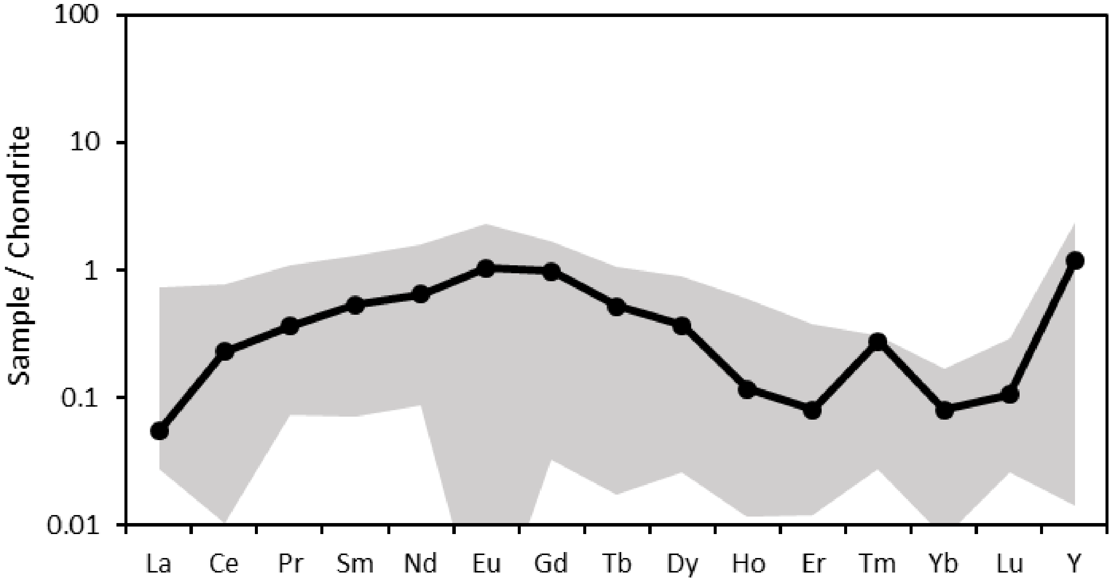

Figure 25. REE patterns from the Gordonsville Mine, Tennessee, from Mao et al. (2016), normalized to chondrite values from Taylor and McLennan (1985). The grey area represents the range of values and the data line represents the median value for each element.

6.5.2 English Pennine Deposits

The Pennine Orefield of England consists of two separate MVT deposits located about 200 km apart, the North and South Pennine Orefields, of which the South Orefield is known for producing the famous "Blue John" banded fluorite. Fluid inclusion studies of fluorite from the South Orefield indicate that the fluorite formed from a fluid similar in temperature and salinity to IKFD fluids. Fluid inclusions yielded salinities from 19–27 weight % NaCl equivalent, while fluid inclusion homogenization temperatures typically range from 90–200°C, with some temperatures as high as 240°C (summarized in Kendrick et al., 2002b). Bau et al. (2003) studied REEs of fluorite from the North and South Orefields; the authors found that REE patterns in carbonate-hosted fluorite from the South Orefield contained negative Ce anomalies and positive Gd and Y anomalies

(Fig. 26), while fluorite from the North Orefield contained no Ce or Gd anomalies but showed large positive Eu anomalies (Fig. 27). REE concentrations in samples from the South Orefield are significantly lower than those from the North Orefield.

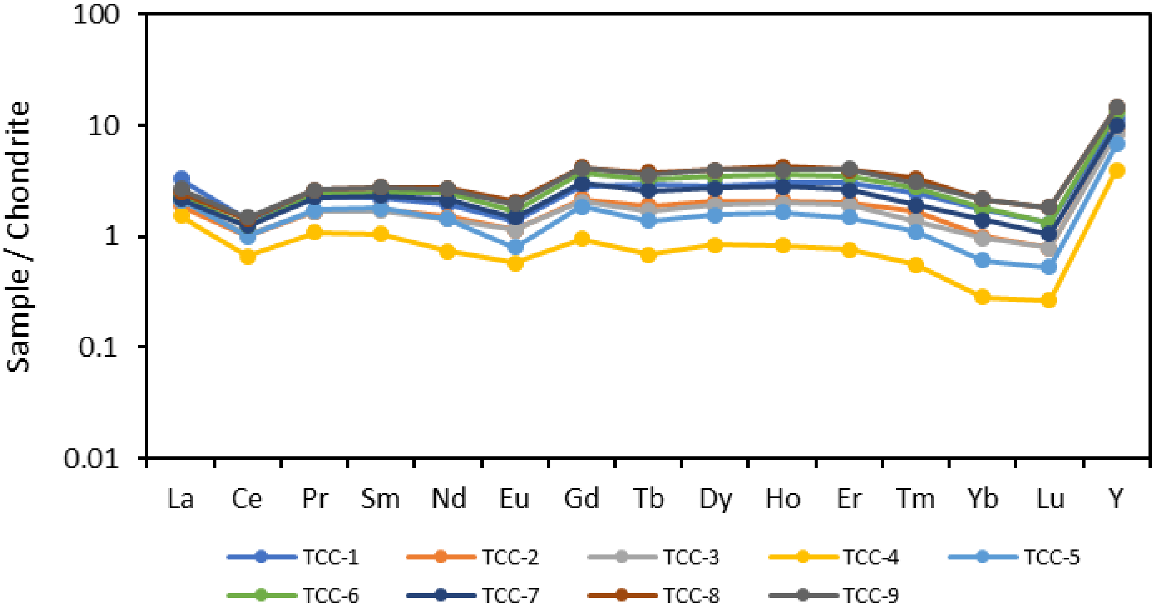

Figure 26. REE patterns of a Blue John fluorite reference sample from the Treak Cliff Cavers - South Pennine Orefield, England, from Bau et al. (2003), normalized to chondrite values from Taylor and McLennan (1985).

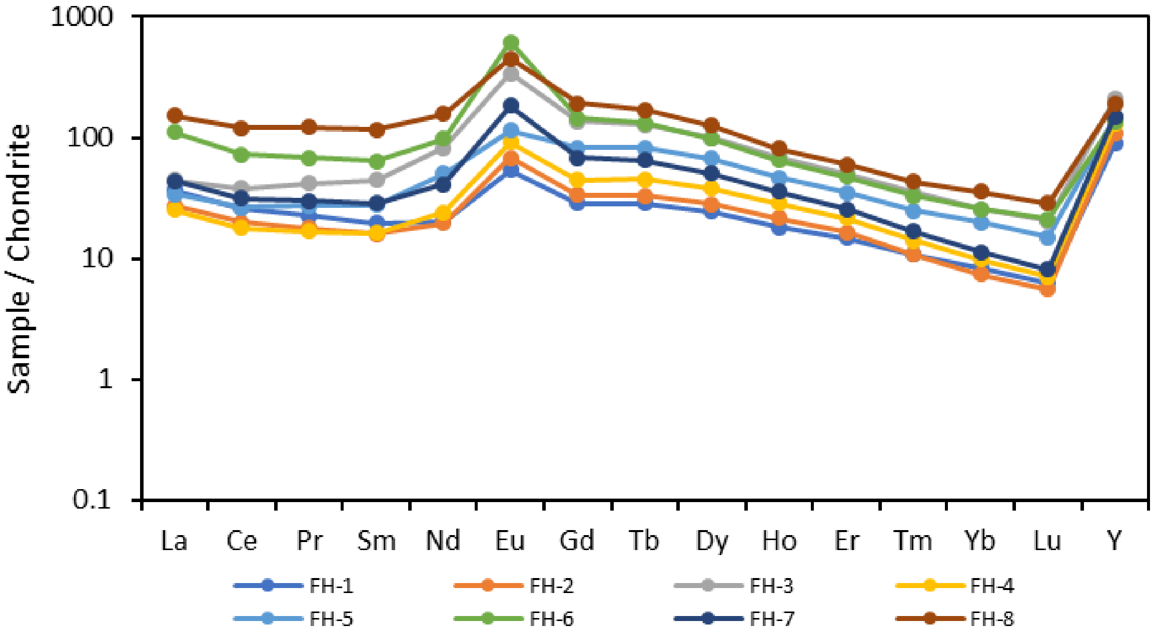

Figure 27. REE patterns of fluorite from the Frazier Hush Mine - North Pennine Orefield, England, from Bau et al. (2003), normalized to chondrite values from Taylor and McLennan (1985).

Bau and Möller (1992) determined that at temperatures at or above 200°C and at pressures of 0.5 Kbar, Eu^{2+} dominates over Eu^{3+} in solution. The Eu^{3+}/Eu^{2+} redox potential in hydrothermal fluids is dependent on pressure, pH, REE speciation, and temperature, with temperature being the most important factor (Bau, 1991; Bau and Möller, 1992). Bau et al. (2003) note that the lack of a positive Eu anomaly in South Orefield fluorite agrees with fluid inclusion data that the fluorite formed from a low temperature < 250°C fluid that was never previously heated above the threshold necessary for Eu^{2+} to predominate under the redox conditions of the mineralizing fluid. Bau et al. (2003) believe the positive Eu anomaly in North Orefield fluorite is indicative of fluids that were heated above temperatures where Eu^{2+} predominates, allowing Eu to decouple from the other trivalent REEs, resulting in an overall increase of Eu in the hydrothermal fluid relative to the other REEs. It is believed that the higher temperature North Orefield fluids originated from deeper crustal levels than the South Orefield (Bau et al., 2003) and evidence indicates that the fluids were enriched in fluorine through interactions with Paleozoic igneous rocks during hydrothermal circulation (Bouch et al., 2006).

South Orefield fluorite is similar to early F1 fluorite from the IKFD in its overall concentrations, slight positive at Gd, and flatter negative HREE slopes. The two differ in that IKFD fluorite analyzed in this study has no distinct negative Ce or Eu anomalies and is LREE depleted. North Orefield fluorite share several similarities to later F2 fluorite from the IKFD. REE patterns between the two are similar, with North Orefield fluorite having higher overall concentrations, more prominent positive Eu anomalies, and no LREE depletion compared to later F2 fluorite from the IKFD, but MREE and HREE patterns are very similar between the two districts. It appears that North Orefield fluorite formed from a higher temperature fluid than either F1 or F2 fluids responsible for IKFD fluorite mineralization, which likely contributed to the larger positive Eu anomaly in North Orefield fluorite compared to IKFD fluorite.

Fluid inclusion data for IKFD fluorite indicate that both F1 and F2 fluids were too cool to produce a positive Eu anomaly in the mineralizing fluid at the site of ore deposition without extremely low oxygen fugacity (Bau and Möller, 1992; Taylor et al., 1992; Spry and Fuhrmann, 1994). However, if F2 fluids originated from the Cambrian Mt. Simon Sandstone aquifer, the basal sandstone lying uncomfortably on Precambrian basement, the fluids would have been exposed to higher temperatures before rising along faults and cooling to the approximately 150°C temperatures found in late fluorite fluid inclusions. Additional evidence supporting this hypothesis is the occurrence of 180–250°C fluid inclusion homogenization temperatures cited to occur within sparry dolomite cement, less than 150 m above the Mt. Simon Sandstone (Leach et al., 1997). Due to divalent Eu's larger ionic radii (1.17 Å) not allowing substitutions for Ca^{2+} (1.00 Å) in the structure of many carbonate minerals (Bau, 1991), any hydrothermal carbonate mineralization prior to the formation of fluorite from a Eu^{2+} rich fluid would increase the concentration of Eu in the fluid. Then as fluids rose along faults and deposited fluorite, the REE composition of the fluid was recorded in the fluorite.

If elevated temperatures are the primary source of the positive Eu anomaly in paragenetically later F2 fluorite, than F1 fluids likely originated in a stratigraphically higher, cooler aquifer than F2 fluids, such as the Ordovician St. Peter Sandstone. The St. Peter Sandstone was modeled to have reached a maximum burial depth of 3,300 m and a maximum temperature of around 140°C in the late Paleozoic, and the Mississippian carbonates that host IKFD mineralization would have been approximately 1200 m above the St. Peter Sandstone (Pitman et al., 1997). Modeling by Pitman and others (1997) agrees with the evidence that F1 fluids from the St. Peter Sandstone would not have reached temperatures as high as fluids from within the Mt. Simon Sandstone, and these lower temperatures may not have been hot enough or had low enough oxygen fugacity to stabilize Eu^{2+}, resulting in the lack of a positive Eu anomaly in early F1 fluorite. It should be noted however, that Pitman and other's modeling does not account for the increased magmatic heat in the region.

Slight positive La and Gd anomalies, along with negative Ce anomalies in the South Orefield are believed to be a reflection of the ore fluid and not a product of the environment under which fluorite mineralization occurred (Bau et al., 2003). The authors note that Ce's ability to occur as both Ce^{3+} and Ce^{4+} could be used as an indication of redox conditions at the site of ore deposition. Work done by Bilal and Müller (1992) suggests that hydrothermal fluids are unlikely to produce substantial quantities of Ce^{4+} because Ce^{4+}/Ce^{3+} redox equilibrium shifts toward higher oxygen fugacity with increasing temperatures.

Unlike the IKFD, limestone host rock dissolution in the Pennine Orefields is minimal, with most fluorite occurring as open space filling in cavities and fractures (Bau et a., 2003). Bau et al. (2003) found REE patterns of South Orefield fluorite to resemble that of marine sediments and seawater, and the REE patterns could be a reflection of the hydrothermal fluids traveling through limestone beds before reaching the site of ore deposition. In contrast, low Ca/Mg ratios in IKFD fluid inclusions led Pelch et al. (2015) to conclude that IKFD mineralizing fluids were dolomitizing, and therefore could not have travelled long distances through the Mississippian carbonates that host the fluorite mineralization without fluid Ca/Mg ratios equilibrating with calcite.

Noble gas and halogen data of fluid inclusions from the South Orefield are in support of mineralizing fluids originating as seawater (Kendrick et al., 2002b). Br/Cl mol ratio values, similar to values obtained in IKFD fluid inclusions, indicate that mineralizing fluids from both districts acquired salinity by the evaporation of seawater beyond the point of halite saturation (Kendrick et al., 2002b). Kendrick et al. (2002a; 2002b) determined that both IKFD and South Orefield fluids contained I/Cl mol ratios elevated above those attainable by evaporation of seawater, indicating fluids from both districts interacted with I-rich organic matter in sedimentary rocks.

A major difference between South Orefield and IKFD fluids lies in the ^{3}He/^{4}He ratios. IKFD fluids contained approximately 6% mantle helium (Kendrick et al., 2002a), likely sourced from the District's intrusive igneous activity, while the South Orefield contained ^{3}He/^{4}He ratios low enough to exclude the possibility of any magmatic input (Kendrick et al., 2002b). Based on the lack of any LREE enrichment within primary hydrothermal fluorite from the IKFD, it is likely that both F1 and F2 fluids mixed with F-rich magmatic gases, not REE-bearing fluids rising along major FAFC faults (Fig. 30). The gases would have supplied the volatiles necessary to reduce the pH of both F1 and F2 fluids low enough to dissolve large concentrations of fluorine (Plumlee et al., 1995). A lack of magmatic fluids being introduced into the regional MVT system could explain the relatively low REE concentrations found in fluorite across the IKFD for fluorite associated with carbonatite magmatism.

6.6 REE Patterns of Fluorite from the Sparks Hill Diatreme

The Sparks Hill Diatreme is an igneous breccia located north-east of Hicks Dome (Fig. 3). A drill core sample of the diatreme obtained from 990 ft below the surface contains a carbonate clast set in a fine grained igneous matrix (Fig. 28). Within the sample is a mineralized fracture that propagates through the igneous matrix and carbonate clast. The fracture is mineralized with purple fluorite through the carbonate clast, and at the boundary of the clast it grades into clear fluorite, and pyrite fills the fracture in the matrix. Fluorite that I analyzed from this sample is characterized by LREE enrichment (Fig. 9) unlike fluorite samples from the rest of the District; like fluorite precipitated from F1 fluids, fluorite from the Sparks Hill Diatreme also has a positive Gd anomaly.

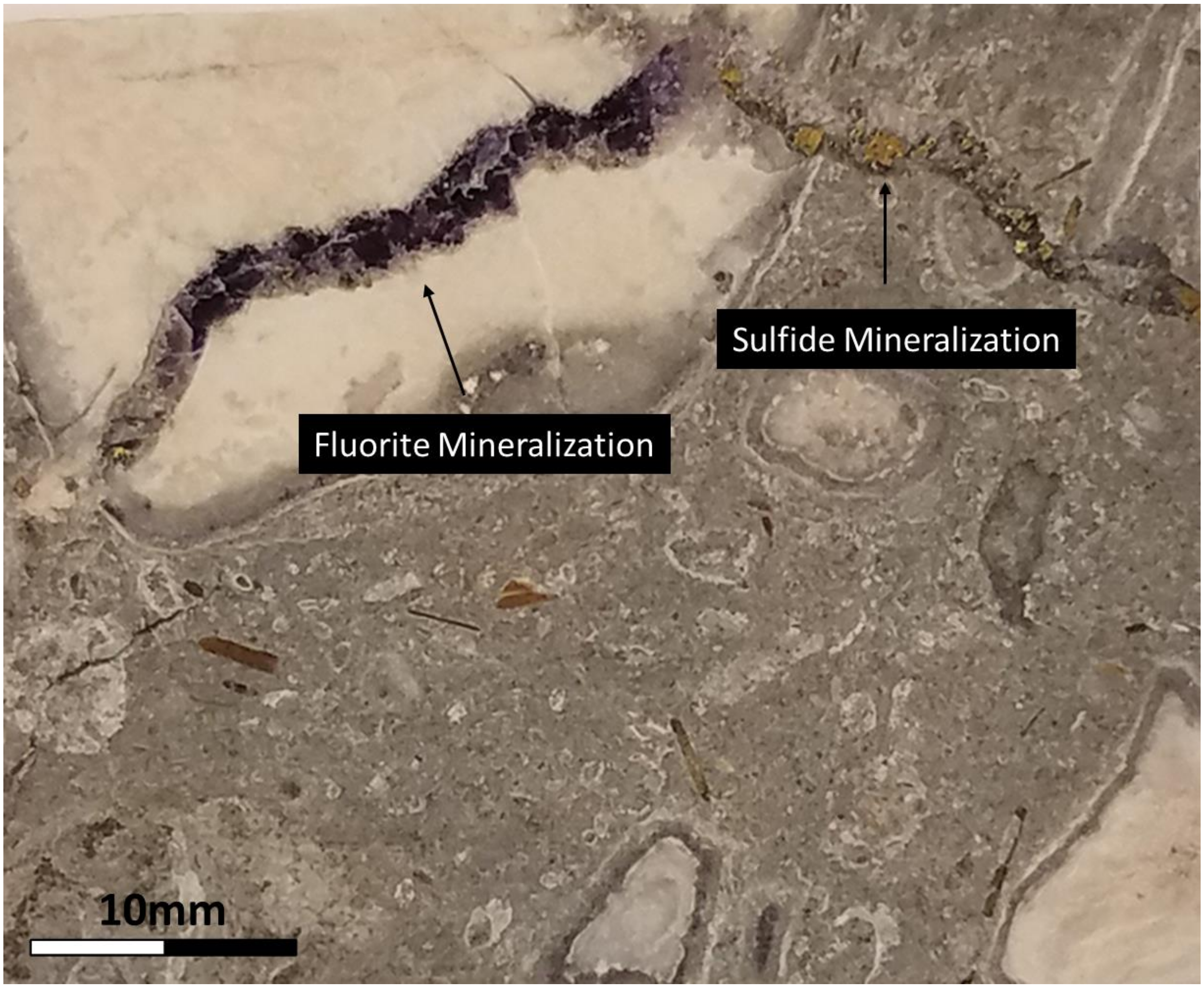

Figure 28. Sample of the Sparks Hill Diatreme showing a mineralized fracture; the fracture is filled with fluorite through the dolostone clast, then it bends and cuts across a brecciated matrix where it is filled with sulfide. Note that the cross-cutting relations of the fracture mean that fracturing and fluorite mineralization must post-date brecciation.

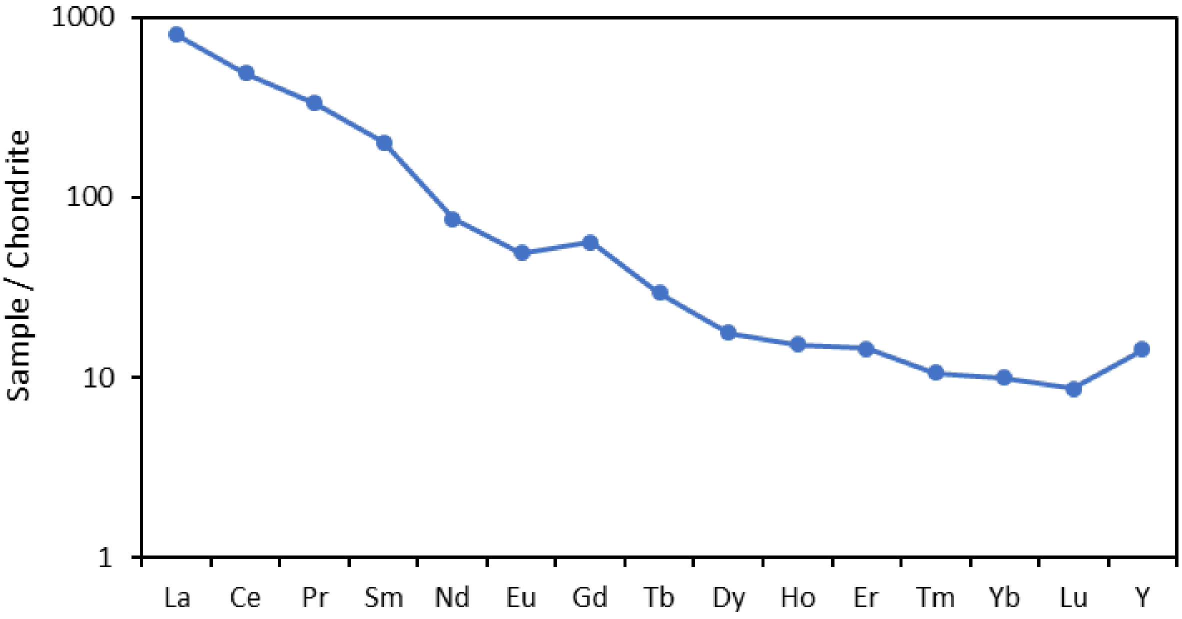

Figure 29. Whole-rock REE pattern of the Sparks Hill Diatreme, from Denny et al. (2015), normalized to chondrite values from Taylor and McLennan (1985).

Denny et al. (2015) identified the presence of micrometer-scale, secondary growths of the REE-fluorocarbonate mineral synchysite [$Ca(Ce, La, Nd, Y)(CO3)_2F$] within the diatreme. Several observations suggest a secondary remobilization and enrichment of REEs into a fluid phase out of the intrusive dikes and diatremes during their alteration; the intrusions show extensive alteration by hydrothermal fluids. First, this sample has post-emplacement fracture filling and mineralization, second, the whole-rock LREE-enriched pattern is similar to that of the District's other intrusive rocks, and third, the occurrence of secondary REE mineralization is present in this and other intrusive rocks throughout the District. Secondary remobilization and enrichment of REEs in a fluid phase that subsequently precipitated fluorite and REE-fluorocarbonate would explain the open space filling of dissolution cavities by fluorite and intergrown REE mineralization in several IKFD intrusive rocks (Moorehead, 2013), in addition to the LREE enrichment of fluorite within the diatreme.

6.7 Fluorite Mineralization at Hicks Dome

It is difficult to determine the relationship between F1 and F2 mineralizing fluids and the mineralization sequence of fluorite from Hicks Dome as there has been no reported correlation between Hicks Dome fluorite and the established paragenetic sequence across the IKFD, particularly how green fluorite fits into the sequence of mineralization. Green fluorite is common towards the surface of Hicks Dome, while fluorite mineralization in the Hicks Dome breccia body from 1600 ft and lower is predominantly purple to clear, commonly intergrown with siliceous material (Brown et al., 1954), and contains an abundance of REE-, Th-, Nb-, and Be-bearing mineralization (Trace, 1960; Hall and Heyl, 1968; Baxter and Bradbury, 1980).

Surprisingly, REE concentrations from the Rose Mine are not significantly elevated and are not even the highest found in the samples analyzed across the District in this study (Fig. 8). One explanation for the "non-uniqueness" of fluorite from the Rose Mine could be that there was no "geometric, geologic, mineralogic, or genetic continuity" found to exist between the Rose Mine breccia and the Hicks Dome breccia (U.S. Geological Survey, 1978), which could explain the abundance of green fluorite and a lack of REE-bearing phases intergrown with Rose Mine fluorite. Spry and Fuhrmann (1994) found fluid inclusion salinities of Rose Mine fluorite to range from 19.7–20.7 weight % NaCl equivalent and fluid inclusion homogenization temperatures to be the highest of all locations sampled throughout the District (≤168°C), with the exception of breccia cemented fluorite obtained from the Hicks Dome breccia (~175°C) (Cunningham and Heyl, 1980). Rose Mine fluorite REE patterns appear to be an intermediate between early and later fluorite patterns from elsewhere in the District. There are no distinct positive Gd or Eu anomalies (Fig. 20, fluorites 1 through 8) that would be indicative of early F1 or later F2 fluorite, and the lack of HREE depletion is also not sufficient to differentiate fluorite formed from either F1 or F2 fluids. Yellow fluorite has been reported to occur in the Rose Mine breccia (U.S. Geological Survey, 1978) and is indicative of early F1 fluorite throughout the rest of the District; however, none was available for analysis in this study. Analyses 9 through 13 of Rose Mine fluorite resemble early F1 fluorite REE patterns, however analysis of samples with low REE concentrations (0.1 x chondrite or less) have shown the most erratic element behavior. Some of the elemental variability and scattering that is common in the low REE samples is likely the result of how the analytical software creates an average value for a series of ablations across a given time frame, essentially making a ratio out of a “noisy” low concentration signal, where the error is large relative to the mean. In addition, average Sr concentrations in all Rose Mine samples are lower compared to the overall higher concentrations of Sr in early F1 fluorite from bedding replacement deposits (Fig. 13). Fluid inclusion temperatures and salinities are more indicative of the F2 fluid; however, this is complicated by the presence of higher temperature mineralizing fluids at Hicks Dome (Spry and Fuhrmann, 1994).

The evidence presented here indicates that fluorite from the Rose Mine breccia is closely related to fluorite mineralization throughout the rest of the District, and unlike fluorite from the deep-seated breccia underneath Hicks Dome, it’s REE chemistry shows that it did not mineralize directly from a release of an orthomagmatic volatile phase. Although fluorite has been found to form directly from low temperature (<200°C) orthomagmatic fluids and orthomagmatic fluids diluted by meteoric water in other deposits throughout the world (e.g., Okorusu, Namibia: Bühn et al., 2002; Amba Dongar, India and Speewah, Australia: summarized in Alvin et al., 2004), these locations are characterized primarily by fluorite with LREE enrichment and high LREE/HREE ratios similar to that of the associated carbonatite rocks. Fenites are also a prominent feature in carbonatite related deposits, where alkali-rich fluids exsolved from the carbonatite magma alter the surrounding country rock to form alkali-bearing minerals such as aegirine, alkali-amphibole, nepheline, phlogopite, alkali-feldspar, and carbonates (summarized in Verplanck et al., 2016). Fenitization of country rocks has not been described within the IKFD.

Evidence points towards a model for which the mineralization within the Hicks Dome breccia occurred from the carbonatite volatile phase that explosively uplifted Hicks Dome and brecciated rocks from the top of Precambrian basement through to the now exposed surface of the dome. A substantial amount of hot carbonatite gases, in addition to carbonatite fluids enriched in REEs, likely mixed with sedimentary brines during the time of brecciation, and as fluids began cooling, they reacted with and cemented carbonate breccia clasts with fluorite, barite, calcite, quartz, sphalerite, galena, and REE-bearing minerals. The mineralization here seems to be isolated from the rest of the District as all primary hydrothermal fluorite analyzed in this study throughout the District is LREE depleted, with no known intergrown REE-bearing phases. The isolated formation of the Hicks Dome breccia mineralization is also supported by the occurrence of the thorium-derived lead isotope, ^{208}Pb, in a galena sample from the Hicks Dome breccia (Heyl et al., 1974). This isotope is not present in other galena samples throughout the rest of the District (Heyl et al., 1974). Other, widespread intrusive igneous activity underlying the District likely supplied magmatic gases and heat into the regional basinal brines (Plumlee et al. 1995), with the intrusive activity under Hicks Dome creating a regional thermal zonation (Fig. 30). If, however, there was mixing between magmatic fluids and the regional basinal brines, magmatic fluids expelled from underneath Hicks Dome were significantly depleted in LREEs from the extensive, presumably earlier REE mineralization in the Hicks Dome breccia.

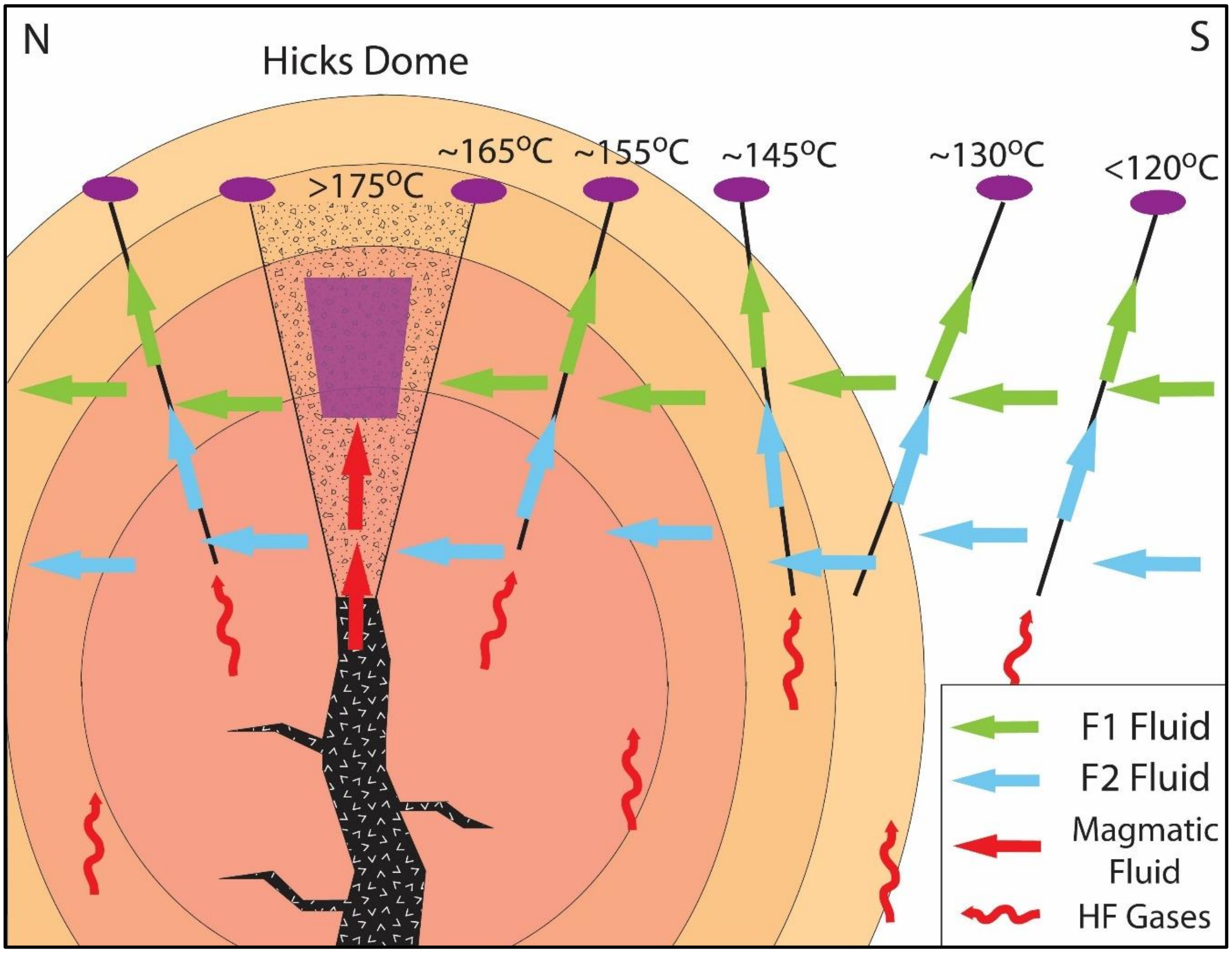

Figure 30. Cartoon illustrating the formation of vein, bedding replacement, and breccia-hosted fluorite mineralization within the IKFD. Purple ovals represent IKFD mineralization, green arrows represent F1 fluids, blue arrows represent F2 fluids, straight red arrows represent magmatic fluids, and curved red arrows represent magmatic gases rising along major FAFC faults (modified from Plumlee et al., 1995). Variation in regional temperatures based on fluid inclusion homogenization temperatures (Taylor et al., 1992). See text for discussion.

6.8 A Model for IKFD Mineralization

A model for IKFD fluorite mineralization, consistent with the new REE data obtained in this study, could be described in a sequence of events as follows:

- Uplift of the Appalachian-Ouachita orogen to the south of the Reelfoot Rift creates a topographic head that drives connate brines in Cambrian and Ordovician aquifers northward and outward through the Reelfoot Rift, and into and across the Illinois basin.
- Extension within the Reelfoot Rift allows for decompression melting of the mantle and ultramafic melts intrude Precambrian basement along the axis of the District. Through partial melting and metasomatism of the mantle, a carbonatite magma forms and rises up below what is now Hicks Dome.
- Pipes, dikes, and diatremes intrude to the surface throughout the District while the carbonatite magma below Hicks Dome releases volatiles that explode upwards to the surface, uplifting 4000 feet of sedimentary rock, fracturing rock from the top of the Precambrian basement up through to the surface, and forming Hicks Dome.
- Hot gases and fluids expelled from the carbonatite magma during the formation of the Hicks Dome breccia locally mix with basinal brines within the brecciated country rocks where they begin to cool, react with carbonate breccia clasts, and deposit fluorite, barite, calcite, quartz, sphalerite, galena, and REE-bearing minerals.
- Magmatic volatiles and fluorine released from intrusive rocks underlying the entire District rise along major FAFC faults where they dissolve into the northward migrating basinal brines, drastically decreasing fluid pH while supplying fluorine.
- F1 fluids from the St. Peter Sandstone begin rising along faults until reaching open spaces where fluid boiling, cooling, and interactions with carbonate wall rocks neutralize fluids,

decrease fluorine solubility, and dissolve sedimentary carbonate so that fluorite begins to mineralize. Some fluids rise along faults that are pinched out and capped by impermeable shale; pressure builds and fluids are forced out laterally through more permeable beds. Fluids migrating laterally through beds that contain pure carbonate begin dissolving large amounts of carbonate, leaving in its place alternating bands of fluorite. In some locations, carbonate dissolution is extensive enough that overlaying formations slump and collapse into the open void space where these solution-slump breccias are cemented with fluorite mineralization.

- As mineralizing fluids continue moving northward closer to the Hicks Dome thermal high, the fluids begin cooling less as they rise up along faults and reach sites of ore deposition. The mineralizing fluids also begin altering the regional intrusive rocks as they continue migrating through the district. The alteration of the intrusive rocks also results in the remobilization of REEs; where the remobilized REEs are reprecipitated in secondary fluorite and as REE-bearing minerals in fractures and dissolution cavities.
- Fluorite mineralization from F1 fluids occurs from yellow 1 through purple 3 with sulfide mineralization taking place in areas of localized reduced sulfur. After the formation of purple 3 fluorite, the mineralizing fluid experiences a change as warmer F2 fluids from the Mt. Simon Sandstone move up along major faults. Fluorite continues forming alternating bands of blue, purple, and clear from blue 1 to the end of purple 6.
- Fluorite mineralization begins to cease with the downward infiltration of late-stage $SO4^{2-}$ rich meteoric fluid into the District, characterized by low temperature and salinity. The meteoric fluid begins driving late-stage calcite, barite, and witherite mineralization.
- Mineralization within the IKFD ceases as basinal brines continue moving northward across the Illinois basin toward the Upper Mississippi Valley District.

Chapter 7: Conclusions

Mineralizing fluids responsible for the formation of the IKFD formed as a result of the mixing between MVT basinal brines and HF-rich magmatic gases. MVT fluids were injected with fluorine and volatiles all along the axis of the District; mineralizing fluids were not modified and charged with fluorine only at Hicks Dome. Data obtained in this study suggest little REE input from magmatic fluids into the regional MVT system.

Fluorite from the IKFD is characterized by LREE depletion, MREE enrichment, and varying degrees of HREE depletion (compared to standard normalization to chondrite). Overall, concentrations of individual REEs are low, on the order of 10 ppm and less. If low degrees of HREE depletion are to be attributed to input of magmatic fluids into the regional MVT system and not to unmodified basinal brines, then the magmatic fluids were unusually depleted in LREEs, possibly from mineralization of LREE-bearing phases before fluid mixing occurred.

For several locations throughout the District, paragenetically early F1 fluorite and paragenetically later F2 fluorite can be distinguished from one another by differences in their REE patterns, consistent with fluid inclusion evidence that early and later fluorite formed from fluids of differing composition. The positive Eu anomaly in paragenetically later F2 fluorite can be attributed to F2 fluids reaching higher temperatures while migrating through a different aquifer than F1 fluids. Along the fringes of the District, the two distinctive REE patterns are less clear, and further analysis of fluorite from these outlying areas that are of known position within the paragenetic sequence will be needed in order to better understand the relationship between the composition of the mineralizing fluids and the paragenetic sequence at distal deposits.

Secondary fluorite within the Sparks Hill Diatreme was found to have REE patterns similar to whole rock patterns of the diatreme and other intrusive rocks within the IKFD. These patterns of fluorite should be attributed to the secondary remobilization of REEs from the intrusive rocks and enriched into secondary fluorite and REE-bearing minerals during the alteration of the intrusive rocks by regional MVT fluids. Analysis of fluorite from the Hicks Dome breccia could help determine if this diatreme deposit mineralized directly from magmatic volatiles expelled off the underlying carbonatite magma or if the extensive REE mineralization here can be also be attributed to secondary remobilization of REEs out of associated intrusive igneous rocks.

The subtle yet overall decrease in total REE concentrations in fluorite samples with increasing distance to Hicks Dome may not be indicative of magmatic fluid input sourced from under Hicks Dome as has been previously thought, but could be explained in part by the thermal zonation around Hicks Dome and its effects on the stability of REE complexes in hydrothermal fluids. All the data acquired in this study from across the District do not indicate the occurrence of extensive REE-bearing mineralization intergrown with fluorite outside of the Hicks Dome breccia.

References

Alvin, M.P., Dunphy, J.M., and Groves, D.I., 2004, Nature and genesis of a carbonatite-associated fluorite deposit at Speewah, East Kimberley region, Western Australia: Mineralogy and Petrology, v. 80, p. 127–153.

Bain, H.F., 1905, The fluorspar deposits of southern Illinois: U.S. Geological Survey, Bulletin 255, 75 p.

Bastin, E.S., 1931, The fluorspar deposits of Hardin and Pope Counties, Illinois: Illinois Geological Survey, Bulletin 58, 116 p.

Bau, M., 1991, Rare-Earth Element Mobility During Hydrothermal and Metamorphic Fluid Rock Interaction and the Significance of the Oxidation-State of Europium: Chemical Geology, v. 93, p. 219–230.

Bau, M., and Möller, P., 1992, Rare earth element fractionation in metamorphogenic hydrothermal calcite, magnesite and siderite: Mineralogy and Petrology, v. 45, p. 231–246.

Bau, M., Romer, R.L., Lüders, V., and Dulski, P., 2003, Tracing element sources of hydrothermal mineral deposits: REE and Y distribution and Sr-Nd-Pb isotopes in fluorite from MVT deposits in the Pennine Orefield, England: Mineralium Deposita, v. 38, p. 992–1008.

Baxter, J.W., and Bradbury, J.C., 1980, Bertrandite at Hicks Dome, Hardin County, Illinois [USA]: Transactions of the Illinois State Academy of Science, v. 73, p. 1–13.

Bethke, C.M., 1986, Hydrologic constraints on the genesis of the Upper Mississippi Valley mineral district from Illinois basin brines: Economic Geology, v. 81, p. 233–249.

Bethke, C.M., Reed, J.D., and Oltz, D.F., 1991, Long-range petroleum migration in the Illinois Basin: American Association of Petroleum Geologists Bulletin, v. 75, p. 925–945.

Bilal, B.A., and Müller, E., 1992, Thermodynamic study of Ce^{4+}/Ce^{3+} redox reaction in aqueous solutions at elevated temperatures: I. Reduction potential and hydrolysis equilibria of Ce^{4+} in HClO4 solutions: Zeitschrift für Naturforschung, v. 47, p. 974–984.

Bosze, S., and Rakovan, J., 2002, Surface-structure-controlled sectoral zoning of the rare earth elements in fluorite from Long Lake, New York, and Bingham, New Mexico, USA: Geochimica et Cosmochimica Acta, v. 66, p. 997–1009.

Bouch, J.E., Naden, J., Shepherd, T.J., McKervey, J.A., Young, B., Benham, A.J., and Sloane, H.J., 2006, Direct evidence of fluid mixing in the formation of stratabound Pb-Zn-Ba-F mineralisation in the Alston Block, North Pennine Orefield (England): Mineralium Deposita, v. 41, p. 821–835.

Bradbury, J.C., and Baxter, J.W., 1992, Intrusive breccias at Hicks Dome: Illinois State Geological Survey, Circular 550, 23 p.

Brannon, J.C., Cole, S.C., Podosek, F.A., Ragan, V.M., Coveney, R.M., Wallace, M.W., and Bradley, A.J., 1996, Th-Pb and U-Pb dating of ore-stage calcite and Paleozoic fluid flow: Science, v. 271, p. 491–493.

Brannon, J.C., Podosek, F.A., and McLimans, R.K., 1992, Alleghenian age of the upper Mississippi valley zinc lead deposit determined by Rb-Sr dating of sphalerite: Nature, v. 356, p. 509–511.

Brecke, E.A., 1962, Ore genesis of the Cave-In-Rock Fluorspar District, Hardin County, Illinois: Economic Geology, v. 57, p. 499–535.

Brown, J.S., Emery, J.A., and Meyer, P.A., 1954, Explosion pipe in test well on hicks dome, Hardin county, Illinois: Economic Geology, v. 49, p. 891–902.

Bühn, B., Schneider, J., Dulski, P., and Rankin, A.H., 2003, Fluid-rock interaction during progressive migration of carbonatitic fluids, derived from small-scale trace element and Sr, Pb isotope distribution in hydrothermal fluorite: Geochimica et Cosmochimica Acta, v. 67, p. 4577–4595.

Burruss, R.C., Richardson, C.K., Grossman, J.N., Lichte, F.E., and Goldhaber, M.B., 1992, Regional and microscale zonation of rare earths elements in fluorite of the Illinois-Kentucky fluorspar district: U.S. Geological Survey Open-File Report 92-1, p. 6-7.

Chesley, J.T., Halliday, A.N., Kyser, T.K., and Spry, P.G., 1994, Direct dating of Mississippi Valley-type mineralization: Use of Sm- Nd in fluorite: Economic Geology, v. 89, p. 1192–1199.

Cluff, R.M., and Byrnes, A.P., 1990, Lopatin analysis of maturation and petroleum generation in the Illinois basin: American Association of Petroleum Geologists Memoir 51, p. 425-45.

Cullers, R.L., and Graf, J.L., 1984, Rare Earth Elements in Igneous Rocks of the Continental Crust: Predominantly Basic and Ultrabasic Rocks: Developments in Geochemistry, v. 2, p. 237–274.

Cunningham, C.G., and Heyl, A.V., 1980, Fluid inclusion homogenization temperatures throughout the sequence of mineral deposition in the Cave-in-Rock area, southern Illinois: Economic Geology, v. 75, p. 1226–1231.

Currier, L.W., and Wagner, O.E., 1944, Geology of the Cave in Rock District: United States Geological Survey, Bulletin 942, 71 p.

Denny, F.B., 2005, The Cottage Grove Dike and mafic igneous intrusions in southeastern Illinois and their relation to regional tectonics and economic resources: M.Sc. thesis, Southern Illinois University at Carbondale, 83 p.

Denny, F.B., Goldstein, A, Devera, J.A., Williams, D.A., Lasemi, Z., and Nelson, W.J., 2008, The Illinois-Kentucky Fluorite District, Hicks Dome, and Garden of the Gods in southeastern Illinois and northwestern Kentucky, in Maria A.H., and Counts, R.C., eds., From the Cincinnati Arch to the Illinois Basin: Geological field excursions along the Ohio River valley: Geological Society of America, Field Guide 12, p. 11–24.

Denny, F.B., Guillemette, R.N., and Lefticariu, L., 2015, Rare earth mineral concentrations in ultramafic alkaline rocks and fluorite within the Illinois-Kentucky Fluorite District: Hicks Dome cryptoexplosive complex, southeast Illinois and northwest Kentucky (USA), in Lasemi, Z., ed., Proceedings of the 47th Forum on the Geology of Industrial Minerals: Illinois State Geological Survey, Circular 587.

Ehya, F., 2012, Variation of mineralizing fluids and fractionation of REE during the emplacement of the vein-type fluorite deposit at Bozijan, Markazi Province, Iran: Journal of Geochemical Exploration, v. 112, p. 93–106.

Emsbo, P., McLaughlin, P.I., Breit, G.N., du Bray, E.A., and Koenig, A.E., 2015, Rare earth elements in sedimentary phosphate deposits: Solution to the global REE crisis?: Gondwana Research, v. 27, p. 776–785.

Fifarek, R.H., Denny, F.B., Snee, L.W., and Miggins, D.P., 2001, Permian igneous activity in southeastern Illinois and western Kentucky; implications for tectonism and economic resources: Abstracts with Programs - Geological Society of America, v. 33, p. 420.

Garven, G., Ge, S., Person, M.A., and Sverjensky, D., 1993, Genesis of Stratabound Ore Deposits in the Midcontinent Basins of North America. 1. The Role of Regional Groundwater Flow: American Journal of Science, v. 293, p. 497–568.

Gernon, T.M., Brown, R.J., Tait, M.A., and Hincks, T.K., 2012, The origin of pelletal lapilli in explosive kimberlite eruptions: Nature Communications, v. 3.

Goldhaber, M.B., Rowan, E., Hatch, J., Zartman, R., Pitman, J., and Reynolds, R., 1994, The Illinois basin as a flow path for low temperature hydrothermal fluids [abs.]: Society of Economic Paleontologists and Mineralogists Research Conference, Lake Ozark, Missouri, May 21, 1994, Abstracts, p. 29-31.

Goldstein, A., 1997, The Illinois-Kentucky fluorite district: The Mineralogical Record, v. 28, p. 3–49.

Gratz, J.F., and Misra, K.C., 1987, Fluid inclusion study of the Gordonsville zinc deposit, central Tennessee: Economic Geology, v. 82, p. 1790–1804.

Grogan, R.M., 1949, Structures due to volume shrinkage in the bedding-replacement fluorspar deposits of Southern Illinois: Economic Geology, v. 44, p. 606–616.

Hall, W.E., and Friedman, I., 1963, Composition of fluid inclusions, Cave-in-Rock fluorite district, Illinois, and upper Mississippi valley zinc-lead district: Economic Geology, v. 58, p. 886–911.

Hall, W.E., and Heyl, A.V., 1968, Distribution of minor elements in ore and host rock, Illinois-Kentucky fluorite district and upper Mississippi valley Zinc-Lead District: Economic Geology, v. 63, p. 655–670.

Hayes, T.S., and Anderson, W.H., 1992, Regionwide correlation of the hydrothermal paragenesis of the Illinois-Kentucky fluorspar district: U.S. Geological Survey Open-File Report 92-1, p. 19-22.

Heyl, A.V., Landis, G.P., and Zartman, R.E., 1974, Isotopic evidence for the origin of Mississippi Valley-type mineral deposits: A review: Economic Geology, v. 69, p. 992–1006.

Kendrick, M.A., Burgess, R., Leach, D., and Pattrick, R.A.D., 2002a, Hydrothermal fluid origins in Mississippi Valley-type ore districts: Combined noble gas (He, Ar, Kr) and halogen (Cl, Br, I) analysis of fluid inclusions from the Illinois-Kentucky fluorspar district, Viburnum

Trend, and Tri-State districts, midcontinent United States: Economic Geology, v. 97, p. 453–469.

Kendrick, M.A., Burgess, R., Pattrick, R.A.D., and Turner, G., 2002b, Hydrothermal fluid origins in a fluorite-rich Mississippi Valley-type district: Combined noble gas (He, Ar, Kr) and halogen (Cl, Br, I) analysis of fluid inclusions from the South Pennine ore field, United Kingdom: Economic Geology, v. 97, p. 435–451.

Kolata, D.R., and Nelson, W.J., 1991, Tectonic history of the Illinois basin, in Leighton, M.W., Kolata, D.R., Oltz, D.F., and Eidel, J.J., eds., Interior cratonic basins: American Association of Petroleum Geologists Memoir, 51, p. 263-286.

Leach, D.L., Apodaca, L.E., Repetski, J.E., Powell, J.W., and Rowan, E.L., 1997, Evidence for hot Mississippi Valley-type brines in the Reelfoot rift complex, south-central United Sates, in Late Pennsylvanian-Early Permian: US Geological Survey Professional Paper, 1577.

Leach, D.L., Taylor, R., Fey, D., and Diehl, S., 2010, A Deposit Model for Mississippi Valley-Type Lead-Zinc Ores: Mineral Deposit Models for Resource Assessment, Chapter A, p. 1–43.

Loges, A., Migdisov, A.A., Wagner, T., Williams-Jones, A.E., and Markl, G., 2013, An experimental study of the aqueous solubility and speciation of Y(III) fluoride at temperatures up to 250°C: Geochimica et Cosmochimica Acta, v. 123, p. 403–415.

Mao, M., Simandl, G.J., Spence, J., Neetz, M., and Marshall, D., 2016, Trace element composition of fluorite and its potential use as an indicator in mineral exploration, in

Geological Fieldwork, 2015, British Columbia Ministry of Energy and Mines: British Columbia Geological Survey Paper 2016-1, p. 181-206.

Migdisov, A.A., and Williams-Jones, A.E., 2014, Hydrothermal transport and deposition of the rare earth elements by fluorine-bearing aqueous liquids: Mineralium Deposita, v. 49, p. 987–997.

Migdisov, A.A., Williams-Jones, A.E., and Wagner, T., 2009, An experimental study of the solubility and speciation of the Rare Earth Elements (III) in fluoride- and chloride-bearing aqueous solutions at temperatures up to 300 °C: Geochimica et Cosmochimica Acta, v. 73, p. 7087–7109.

Moorehead, A., 2013, Igneous intrusions at Hicks Dome, southern Illinois, and their relationship to fluorine-base metal-rare earth element mineralization: M.Sc. thesis, Southern Illinois University Carbondale, 223 p.

Nelson, W.J., 1991, Structural styles of the Illinois basin: American Association of Petroleum Geologists Memoir 51, p. 209-243.

Nelson, W.J., 1995, Structural Features in Illinois: Illinois State Geological Survey Bulletin 100, 144 p.

Pelch, M.A., Appold, M.S., Emsbo, P., and Bodnar, R.J., 2015, Constraints from fluid inclusion compositions on the origin of Mississippi valley-type mineralization in the Illinois Kentucky district: Economic Geology, v. 110, p. 787–808.

Pitman, J.K., Goldhaber, M.B., and Spoetl, C., 1997, Regional diagenetic patterns in the St. Peter Sandstone; implications for brine migration in the Illinois Basin: U.S. Geological Survey Bulletin, p. A1–A17.

Plumlee, G.S., Goldhaber, M.B., and Rowan, E.L., 1995, The potential role of magmatic gases in the genesis of Illinois-Kentucky fluorspar deposits: implications from chemical reaction path modeling: Economic Geology, v. 90, p. 999–1011.

Potter, C.J., Goldhaber, M.B., Heigold, P.C., and Drahovzal, J.A., 1995, Structure of the Reelfoot-Rough Creek rift system, Fluorspar area fault complex, and Hicks Dome, southern Illinois and western Kentucky - new constraints from regional seismic reflection data: U.S. Geological Survey Professional Paper, v. 1538.

Rakovan, J., 2006, A Word to the Wise: Mississippi Valley-Type Deposits: Rocks and Minerals, v. 81, p. 69-71.

Reynolds, R.L., Goldhaber, M.B., and Snee, L.W., 1997, Paleomagnetic and ^{40}Ar/^{39}Ar from the Grant intrusive breccia and comparison to the Permian Downeys Bluff Sill—Evidence for Permian igneous activity at Hicks Dome, southern Illinois: U.S. Geological Survey, Bulletin 2094-G, 16 p.

Richardson, C.K., and Holland, H.D., 1979, Fluorite deposition in hydrothermal systems: Geochimica et Cosmochimica Acta, v. 43, p. 1327–1335.

Richardson, C.K., and Pinckney, D.M., 1984, The chemical and thermal evolution of the fluids in the Cave-in-Rock fluorspar district, Illinois; Mineralogy, paragenesis, and fluid inclusions: Economic Geology, v. 79, p. 1833–1856.

Richardson, C.K., Rye, R.O., and Wasserman, M.D., 1988, The chemical and thermal evolution of the fluids in the Cave-in-Rock fluorspar district, Illinois: Stable isotope systematics at the Deardorff mine: Economic Geology, v. 83, p. 765–783.

Rowan, E.L., and Goldhaber, M.B., 1996, Fluid inclusion and biomarker measurements in the Upper Mississippi Valley Zn-Pb district: Implications for the fluid flow and thermal history of the Illinois basin: U.S. Geological Survey Bulletin, 2094-F.

Rowan, E.L., and de Marsily, G., 2001, Infiltration of Late Paleozoic evaporative brines in the Reelfoot rift: a possible salt source for Illinois basin formation waters and MVT mineralizing fluids: Petroleum Geoscience, v. 7, p. 269–279.

Ruiz, J., Richardson, C.K., and Patchett, P.J., 1988, Strontium isotope geochemistry of fluorite, calcite, and barite of the Cave-in-Rock fluorite district, Illinois: Economic Geology and the Bulletin of the Society of Economic Geologists, v. 83, p. 203–210.

Schwinn, G., and Markl, G., 2005, REE systematics in hydrothermal fluorite: Chemical Geology, v. 216, p. 225–248.

Sheard, E.R., Williams-Jones, A.E., Heiligmann, M., Pederson, C., and Trueman, D.L., 2012, Controls on the concentration of zirconium, niobium, and the rare earth elements in the

Thor Lake rare metal deposit, Northwest Territories, Canada: Economic Geology, v. 107, p. 81–104.

Snee, L.W., and Hayes, T.S., 1992, ^{40}Ar/^{39}Ar geochronology of intrusive rocks and Mississippi-Valley type mineralization and alteration from the Illinois- Kentucky fluorspar district [extended abs.]: U.S. Geological Survey Open- File Report 92-1, p. 59-61.

Spry, P.G., and Fuhrmann, G.D., 1994, Additional fluid inclusion data for the Illinois-Kentucky fluorspar district: evidence for the lack of a regional thermal gradient: Economic Geology, v. 89, p. 288–306.

Spry, P.G., Koellner, M.S., Richardson, C.K., and Jones, H.D., 1990, Thermochemical changes in the ore fluid during deposition at the Denton mine, cave-in-rock fluorspar district, Illinois: Economic Geology, v. 85, p. 172–181.

Symons, D.T.A., 1994, Paleomagnetism and the late Jurassic genesis of the Illinois-Kentucky fluorspar deposits: Economic Geology, v. 89, p. 438–449.

Taylor, S.R., and McLennan, S.M., 1985, The Continental Crust: Its Composition and Evolution: Blackwell Scientific Publications, Oxford, 312 p.

Taylor, C.D., Rowan, E.L., Goldhaber, M.B., and Hayes, T.S., 1992, A relationship between Hicks Dome and temperature zonation in fluorite in the Illinois-Kentucky district—a fluid inclusion study [extended abs.]: U.S. Geological Survey Open-File Report 92-1, p. 62-64.

Trace, R.D., 1960, Significance of unusual mineral occurrence at Hicks Dome, Hardin County, Illinois: U.S. Geological Survey Professional Paper 400-B, p. B63-B64.

U.S. Geological Survey, 1978, Office of Mineral Exploration Report 6873: U.S. Geological Survey.

U.S. Geological Survey, 2014, Mineral commodity summaries 2014: U.S. Geological Survey, 196 p.

Van Schmus, W.R, Bickford, M. E., and Turek, A., 1996, Proterozoic geology of the east-central Midcontinent basement, in Van der Pluijm, B.A, and Catacosinos, P.A., eds., Basement and Basins of Eastern North America: Boulder, Colorado, Geological Society of America Special Paper 308.

Verplanck P.L., Mariano, A.N., and Mariano, A. Jr., 2016, Rare earth element ore geology of carbonatites: Reviews in Economic Geology, 18:5-32.

Verplanck, P.L., Van Gosen, B.S., Seal, R.R., and McCafferty, A.E., 2014, A Deposit Model for Carbonatite and Peralkaline Intrusion-Related Rare Earth Element Deposits: Mineral Deposit Models for Resource Assessment, 58 p.